Hemin availability induces coordinated DNA methylation and gene expression changes in *Porphyromonas gingivalis*

Ricardo Costeira[1¶], Joseph Aduse-Opoku[2¶], Jon J Vernon[3], Francisco Rodriguez-Algarra[4], Susan Joseph[2], Deirdre A Devine[3], Philip D Marsh[3], Vardhman Rakyan[4], Michael A Curtis[2*^], Jordana T Bell[1*^]

[1]Department of Twin Research and Genetic Epidemiology, King's College London, London SE1 7EH, UK
[2]Centre for Host-Microbiome Interactions, Faculty of Dentistry, Oral & Craniofacial Sciences, King's College London, London SE1 9RT, UK
[3]Division of Oral Biology, School of Dentistry, University of Leeds, Leeds LS2 9LU, UK
[4]The Blizard Institute, Barts and The London School of Medicine and Dentistry, Queen Mary University of London, London E1 2AT, UK

* Corresponding authors
Email addresses: jordana.bell@kcl.ac.uk, mike.curtis@kcl.ac.uk

¶ These authors contributed equally to this work
^ These authors also contributed equally to this work

Short title: DNA methylation and expression in *P. gingivalis*

Word count: 8228 words

Abstract

Periodontal disease is a common chronic inflammatory disease driven by the sub-gingival microbiota. *Porphyromonas gingivalis* is an important bacterium in the development of the disease that expresses a variety of virulence determinants. The environmental concentration of hemin, an essential nutrient of this organism, is a global regulator of virulence in *P. gingivalis*: high levels of hemin lead to increased expression of several virulence determinants. However, the mechanism through which hemin influences bacterial gene expression is poorly understood. Bacterial epigenetic processes, primarily DNA methylation, have the potential to fulfil this mechanistic role. Here, we characterised the methylome of *P. gingivalis*, and compared its variation to transcriptomic changes in response to changes in hemin concentration.

Gene expression and DNA methylation profiling of *P. gingivalis* W50 was performed, following continuous culture in chemostats with excess or limited hemin, using Illumina RNA-Seq and Nanopore DNA sequencing. DNA methylation quantification was carried out for N6-methyladenine (6mA) and 5-methylcytosine (5mC) base pair modifications. Differential expression and differential methylation in response to excess hemin availability are presented after multiple testing correction (FDR 5%).

In excess hemin there were 161 over- and 268 under-expressed genes, compared to limited hemin culture. Genes under-expressed in excess hemin were involved in iron recruitment (the hemophore HmuY) and transport (TonB-dependent receptors), and those over-expressed were involved in Fe-S and 4FE-4S cluster binding, and metal cluster binding. Hemin-dependent differentially methylated signals were observed for both 6mA and 5mC, with 49 and 47 signals, respectively. Coordinated genome-wide differential expression and methylation effects were observed in 6 genes, a Ppx/GppA family phosphatase, a lactate utilization protein, 4-alpha-glucanotransferase, two ABC transporter proteins, and a hypothetical protein HMPREF1322_RS00730. The findings indicate that altered genome methylation occurs in response to the availability of hemin and give insights into the molecular mechanisms of regulation of virulence in this bacterium.

Author Summary

DNA methylation has important roles in bacteria, including in the regulation of transcription. *Porphyromonas gingivalis,* an oral pathogen in periodontitis, exhibits well-established gene expression changes in response to hemin availability. However, the gene regulatory processes underlying these effects remain unknown. To this end, we profiled the novel *P. gingivalis* epigenome, and assessed epigenetic and transcriptome variation under limited and excess hemin conditions. As expected, multiple gene expression changes were detected in response to limited and excess hemin conditions. Notably, we also detected differential DNA methylation signatures for both N6-methyladenine (6mA) and 5-methylcytosine (5mC) in response to hemin availability. Joint analyses identified a subset of coordinated changes in gene expression, 6mA, and 5mC methylation that target genes involved in lactate utilization and ABC transporters. The results identify novel regulatory processes underlying the mechanism of hemin regulated gene expression in *P. gingivalis*, with phenotypic impacts on its virulence in periodontal disease.

62 # Introduction

63 Teeth are secured in the mouth through the periodontal ligament, which is attached to the
64 subgingival root surface and the alveolar bone. Periodontal disease is a common chronic
65 inflammatory disease of the periodontal tissues that is driven by bacteria in subgingival microbial
66 biofilms on the root surface. In periodontal disease the integrity of the attachment tissues becomes
67 compromised leading to bleeding, gingival recession, formation of deep periodontal pockets and
68 periodontal bone loss; ultimately culminating in tooth loss in a susceptible host. Periodontitis is a
69 global health issue affecting both developed and developing nations (1, 2). Furthermore,
70 periodontitis is also associated with a range of extra-oral inflammatory conditions, such as diabetes
71 and cardiovascular disease, rheumatoid arthritis, Alzheimer's disease and pregnancy complications
72 (3, 4, 43).

73 During the progression from health to periodontal disease, the oral microbiota undergoes a major
74 transition wherein the microbial community increases in total bacterial diversity, accompanied by a
75 bloom in disease-associated bacteria which start to dominate the community, while being otherwise
76 present in low numbers in healthy microbiota (40). *Porphyromonas gingivalis*, a black-pigmenting
77 anaerobic rod bacterium, is well established as one of the organisms which is positively associated
78 with this shift to a dysbiotic microbiota in disease. Indeed, *P. gingivalis* has been shown to act as a
79 trigger for the conversion of the subgingival microbiota to a more diverse and more pathogenic
80 community in animal models of disease (44, 45). This keystone pathogen behaviour has been
81 attributed to the expression of a variety of extracellular virulence determinants including those
82 trafficked through a Type IX secretion system (T9SS) and through the production of large numbers of
83 outer membrane vesicles, which are collectively able to destabilise the host-microbe homeostasis at
84 this mucosal surface (5-7, 46, 47).

85 Hemin, iron (III) protophophyrin IX chloride, is a major source of iron for a variety of organisms,
86 including *P. gingivalis* where it is an essential supplement for growth. *P. gingivalis* has a dedicated
87 transport system to ensure an efficient accumulation of hemin on the surface for iron utilisation.
88 Subsequent conversion of hemin to μ-oxo bis-haem, and its complexation with iron III, leads to black
89 pigmentation of the bacterial cells, a prominent characteristic of *P. gingivalis* on solid media
90 containing blood (8). *P. gingivalis*, HmuY and HusA are dedicated, surface-exposed hemophore-like
91 proteins that scavenge and bind hemin, free or released from heme containing proteins by gingipain
92 proteases. The complexes deliver the bound heme to outer-membrane receptors for internalization
93 (HmuR or HusB) and heme is then imported through a dedicated TonB-dependent transport
94 machinery (12).

95 The concentration of environmental hemin acts as a regulator of virulence in this bacterium: cells
96 cultured in high concentrations of hemin - comparable to the situation in a diseased periodontium
97 with elevated bleeding - upregulate the expression of a wide variety of virulence
98 determinants,including a range of hydrolytic enzymes such as the gingipain cysteine proteases, and
99 other protein products many of unknown function (23, 24). High-hemin grown cells are significantly
100 more pathogenic in animal models of tissue destruction compared to cell grown under hemin
101 limitation (9-11). Hence the availability of hemin in the growth media is critical to the full expression
102 of virulence of *P. gingivalis* and heme may be regarded as a global regulator of transcription in this
103 bacterium.Although previous studies have characterised the impact of hemin availability on gene
104 expression and virulence in *P. gingivalis*, the regulatory processes underlying these functional
105 changes are not well understood. However, the P. *gingivalis* ATCC33277– genome encodes seven
106 two-component signal transduction system (TCS) pairs of a response regulator and a histidine kinase

107 traditionally involved in gene regulation on other organisms (13). Recently it has been reported that
108 one of these TCS, PorX/PorY, responds to environmental heme and through the co-ordinate action
109 of porX and *sigP* regulates transcription of the T9SS and heme accumulation and mutants defective
110 in either *porX* or *porY* are attenuated in a mouse model of virulence (14, 15). However, given the
111 magnitude of changes in response to the concentration of heme, there may be other mechanisms of
112 heme regulated gene expression in P. gingivalis.

113 Like eukaryotic genomes, bacterial genomes are subject to epigenetic modifications specifically DNA
114 methylation, which has multiple roles in bacteria including the regulation of transcription. Bacterial
115 DNA methylation includes modifications N6-methyladenine (6mA), 5-methylcytosine (5mC), and N4-
116 methylcytosine (4mC), of which 6mA is most prevalent in prokaryotes. Recent development in single
117 molecule sequencing technologies, for example Nanopore sequencing, allow for the detection of
118 these multiple DNA methylation base modifications. Using this approach, bacterial DNA methylation
119 signatures have recently been shown to impact gene expression profiles and genome stability (16,
120 17).

121 In this study, we investigated the impact of hemin availability on the *P. gingivalis* epigenome and
122 transcriptome. *P. gingivalis* W50 was grown in continuous culture to achieve synchronous growth,
123 under either limited heme or excess heme conditions. Subsequently, DNA sequencing using
124 Nanopore and RNA sequencing using Illumina were carried out, to profile the *P. gingivalis* DNA
125 methylome and transcriptome under each condition. Hemin-dependent differentially modified
126 signatures were identified for gene expression, as well as for 6mA and 5mC methylation profiles.
127 Comparison of the signals highlighted a cluster of coordinated changes in 6 genes, including in genes
128 related to lactate utilisation and in ABC transporters.

129

130 Results

131 Gene expression and DNA methylation profiling of *P. gingivalis* W50 was performed after culturing in
132 active chemostat runs with excess (5 mg L^{-1}) or limited hemin (0.2 mg L^{-1}). Biological replicates were
133 collected every 48-hours after achieving steady state, with three biological replicates per
134 experimental condition profiled using Illumina RNA-Seq and Nanopore DNA sequencing technologies
135 (Fig 1).

136 Continuous chemostat environment

137 Steady state was achieved by days 3 and 4 for excess and limited hemin (Fig 2), respectively. Colony
138 counts of *P. gingivalis* W50 were consistently higher in excess hemin culture versus limitation,
139 elevated by an average of 1.52×10^9 (range $3.44 \times 10^8 – 3.07 \times 10^9$) CFU mL^{-1}. OD_{600} ranged between
140 1.67–1.72 (mean 1.69) and 0.357–0.376 (mean 0.367), for excess and limitation respectively. The pH
141 remained stable for both excess and limited hemin culture, 6.9–7.0 and 7.0–7.1 respectively, whilst
142 temperature remained between 36.7 and 37.1°C for both conditions.

143 Gene expression changes

144 RNA-seq data for the six samples was processed using ProkSeq (18) [nd DESeq2 (19) to assess gene
145 expression changes observed after culturing *P. gingivalis* in excess (treatment) and limited (control)
146 hemin conditions. These results are mapped to the *P. gingivalis* W50 genome (RefSeq assembly
147 accession no. GCF_000271945.1). Out of 1,192 total genes analysed, those with an expression LFC >
148 1.5 or LFC < −1.5 were considered differentially expressed after multiple testing correction (FDR =
149 5%).

150 Altogether, 161 and 268 differentially expressed genes (DEGs) were respectively over- and under-
151 expressed in excess hemin across the Pg genome (Fig 3). The 161 DEGs over-expressed in excess
152 hemin included genes encoding homologous proteins of the rubrerythrin family
153 (HMPREF1322_RS04040), 4Fe-4S cluster domain-contain containing proteins
154 (HMPREF1322_RS09700, HMPREF1322_RS04860, HMPREF1322_RS04425), a thiamine phosphate
155 synthase (HMPREF1322_RS02110), electron transport complex subunits (HMPREF1322_RS04875,
156 HMPREF1322_RS04865, HMPREF1322_RS01760, HMPREF1322_RS04880, HMPREF1322_RS04870,
157 HMPREF1322_RS04885, HMPREF1322_RS01765), SDR family/ferredoxin oxidoreductases
158 (HMPREF1322_RS07305, HMPREF1322_RS04445, HMPREF1322_RS04440, HMPREF1322_RS00310)
159 and several dehydrogenases (*e.g.* HMPREF1322_RS07315, HMPREF1322_RS04430 and
160 HMPREF1322_RS06505) (Table 1; S1 Table). Methyltransferases targeting tRNA and 16S rRNA
161 molecules were also over-expressed in excess hemin (HMPREF1322_RS00530,
162 HMPREF1322_RS05610, HMPREF1322_RS04605). Most of these genes encode proteins that contain
163 iron as part of their tertiary structure. Three operonic genes, originally labelled as encoding TapA,
164 TapB and TapC (20), HMPREF1322_RS02140, HMPREF1322_RS02145, HMPREF1322_RS02150,
165 respectively, were also over-expressed. TapA, TapB and TapC contribute to virulence in a mouse
166 model as single isogenic mutants are attenuated. Both TapA and TapC exhibit the C-terminal domain
167 signature typical of the type IX secretion system (T9SS) and are therefore cargo proteins as are the
168 proteases HMPREF1322_RS06795 (PrtT) and Lys-gingipain (Kgp).

169 The 268 DEGs under-expressed in excess hemin included genes *hmuY* (hemin-binding),
170 HMPREF1322_RS06790 (hemin transport), and those encoding homologues of at least 35
171 transposases (*e.g.* HMPREF1322_RS07370, HMPREF1322_RS07285, HMPREF1322_RS10850) (Table
172 2; S2 Table). Other genes under-expressed in excess hemin conditions included genes coding
173 several transporter proteins, with at least eight genes coding ABC transporter proteins (*e.g.*
174 HMPREF1322_RS00745, HMPREF1322_RS00115, HMPREF1322_RS08925). Two genes coding for
175 class I SAM-dependent methyltransferases (HMPREF1322_RS07630, HMPREF1322_RS07185) and
176 one gene coding for an isoprenylcysteine carboxylmethyltransferase family protein
177 (HMPREF1322_RS07190) were under-expressed in excess hemin conditions. The gene encoding the
178 largest protein component of the type IX secretion system (T9SS), Sov (SprA), and also genes
179 encoding OmpH, PorN (GldN) and PorX along with five cargo proteins, are under-expressed in excess
180 hemin (S2 Table).

181 Different types of genes involved in virulence were identified in both the under- and over-expressed
182 DEG subsets. For example, these included difference types of N-acetylmuramoyl-L-alanine amidase
183 genes, T9SS type A sorting domain-containing protein genes, MATE family efflux transporter genes
184 and tetratricopeptide repeat protein genes were identified (S1 and S2 Tables).

185

186 We explored molecular functions shared across the DEGs, although a proportion of genes were not
187 well characterised. Sixty-seven under-expressed (25% of total) and 19 over-expressed (12%) genes
188 identified during growth in excess hemin encoded hypothetical proteins. Additionally, only 16 (6%)
189 of under-expressed genes and 49 (30%) of over-expressed genes identified had well-characterised
190 annotations in RefSeq. A GO term enrichment analysis was carried out using ShinyGO and gene
191 symbols that matched genes in the reference strain *P. gingivalis* W83 (21), with altogether 8 (out of
192 16 well-characterised) under-expressed and 40 (out of 49 well-characterised) over-expressed genes.
193 Forty-two and 43 GO molecular functions were enriched in genes under- and over-expressed
194 respectively in excess hemin conditions. In both cases, molecular functions identified were mostly

195 related to binding activities such as cyclic compound binding, heterocyclic compound binding and
196 ion binding (Fig 4; S3 and S4 Tables). In excess hemin, functions related to Fe-S cluster binding,
197 4Fe-4S cluster binding and metal cluster binding, and several different catalytic activities, including
198 GTPase, metallo-endopeptidase, active transmembrane transporter and diphosphotransferase
199 activities, among others (Fig 4; S4 Table).

200

201 Two sensitivity analyses were carried out for the genome-wide DESeq2 DEG results presented here.
202 A first sensitivity analysis was performed using edgeR, which normalizes expression data differently
203 to DESeq2, and consistently identified the majority of DEGs identified with DESeq2 (S1 Fig).
204 Specifically, edgeR identified 166 genes as over-expressed and 266 genes as under-expressed with
205 excess hemin, of which 161 and 265 were previously identified with DESeq2. In a second general
206 sensitivity analysis, a principal component analysis (PCA) of the genome-wide RNA-seq levels also
207 confirmed overall global differences in gene expression levels between the culturing conditions (S2
208 Fig).

209

210 DNA methylation changes

211 Nanopore sequencing data were generated for the same six biological samples analysed with
212 Illumina RNA sequencing. Methylation levels for 6mA and 5mC were characterised using Tombo with
213 motif-independent 'all-context' models to estimate the proportion of methylated reads at each
214 genomic position, considering only >2M positions with a minimum 10× coverage. PCA of the
215 genome-wide DNA methylation levels pointed to both global 6mA and 5mC differences in *P.*
216 *gingivalis* according to hemin culture conditions (S3-A Fig) and mirrored the PCA pattern observed
217 for gene expression (S1 Fig). Similar results were observed when considering signals with at least
218 100× coverage (S3-B Fig). Differential methylation analyses with respect to hemin levels were then
219 carried out at each adenine and cytosine base position. We only considered signals with at least 5%
220 mean methylation difference between the experimental conditions after multiple testing correction
221 (FDR 5%) for altogether 139,794 adenines and 87,398 cytosines.

222

223 Forty-nine differentially methylated adenine sites (DMAs) were identified between experimental
224 conditions across the *P. gingivalis* genome (Fig 5). A cluster of 15 DMAs was observed in a genomic
225 region (NZ_AJZS01000011.1 ≈ 12 – 20 kb) containing the (Fe-S)-binding protein
226 HMPREF1322_RS00720, lactate utilization protein HMPREF1322_RS00725, hypothetical protein
227 HMPREF1322_RS00730, PaaI family thioesterase HMPREF1322_RS00735 and ABC transporter ATP-
228 binding protein HMPREF1322_RS00740 (Fig 5 top panel, purple; Fig 7). In annotating DMAs to genes,
229 if genes up to ±1 kb away from the DMA on both strands are considered, all DMAs are annotated to
230 at least one gene for a total of 75 genes altogether. Furthermore, 25 DMAs were annotated to genes
231 on the same strand, including seven DMAs encoding a lactate utilization protein
232 (HMPREF1322_RS00725), five in a hypothetical protein (HMPREF1322_RS00730), and two each in a
233 4-alpha-glucanotransferase (HMPREF1322_RS03650) and a Ppx/GppA family phosphatase
234 (HMPREF1322_RS06180) (Table 3). Four DMAs were located within 1 kb of a gene encoding a (Fe-
235 S)-binding protein (HMPREF1322_RS00720). In a sensitivity analysis considering only adenines with
236 at least 100× coverage (85,090 adenines), 20 DMAs were identified at FDR = 5% (S5 Table) and all
237 20 were also identified in the results of the main analysis.

238 Forty-seven differentially methylated cytosines (DMCs) were identified between experimental
239 conditions across the *P. gingivalis* genome (Fig. 5). Two clusters of 15 and 12 DMCs emerged - the
240 first was the same as the DMA cluster region (NZ_AJZS01000011.1, ≈ 12 – 20 kb), and the second
241 was in a genomic region (NZ_AJZS01000050.1, ≈ 0 – 3.5 kb) containing the DUF2436 domain-
242 containing protein HMPREF1322_RS04325 and nucleoside permease HMPREF1322_RS04330 (Fig. 5
243 bottom panel, purple and green; Fig 7). Thirty-five DMCs were located in 16 genes including in genes
244 identified in the DMA analyses above. Specifically, four DMCs were located in genes encoding the
245 (Fe-S)-binding protein HMPREF1322_RS00720, two in the lactate utilization protein
246 HMPREF1322_RS00725, and two in the hypothetical protein HMPREF1322_RS00730 reported
247 immediately above for 6mA. Single DMCs were also identified in the 4-alpha-glucanotransferase
248 HMPREF1322_RS03650 and Ppx/GppA family phosphatase HMPREF1322_RS06180 genes (Table 4).
249 Overall, if genes up to ±1 kb away on both strands are considered, 31 genes harboured DMCs, of
250 which 10 also harboured DMAs. Other genes annotated to the DMCs identified included those
251 encoding transporter proteins such as an iron ABC transporter permease (HMPREF1322_RS01240)
252 and others (HMPREF1322_RS01245; HMPREF1322_RS06460). In sensitivity analysis considering only
253 cytosines with at least 100× coverage (46,930 cytosines), 47 DMCs are also identified, of which 27
254 were also in the main analysis results (S6 Table).

255 We explored evidence for putative DNA sequence motifs at the identified DMAs and DMCs. To this
256 end, we searched for over-representation of up to 15-nucleotide long sequences surrounding all
257 DMAs and DMCs. Although the analyses identified putative sequences of length 10-11 nucleotides,
258 the results did not reach statistical significance (MEME E-value > 0.05; S4 Fig).

259

260 Genes with coordinated differential DNA methylation and expression changes

261 We assessed whether the observed DEGs also exhibited DNA methylation changes for 6mA and 5mC.
262 We first compared DEGs to DMAs and DMCs each (Fig 6), and then explored further genomic regions
263 that contained DEGs, DMAs, and DMCs (Fig. 7).

264 Overall, 23 DEGs also harboured DMAs (Table 5; Table 6). Of these, 8 genes were over-expressed
265 in excess hemin including the SDR family oxidoreductase HMPREF1322_RS07305 (*P. gingivalis* W83:
266 PG2069) and the Ppx/GppA family phosphatase HMPREF1322_RS06180 (W83: PG1739) genes
267 (Table 5). In all 8 cases the DMA was on the same strand as the gene, located either in or upstream
268 of the gene (Table 5), with hypermethylation in excess hemin for most cases. The 15 DEGs with
269 DMAs under-expressed in excess hemin included the hypothetical protein HMPREF1322_RS00730
270 (W83: PG1173) in the lactate utilization cluster, the lactate utilization protein
271 HMPREF1322_RS00725 (W83: PG1172), the 4-alpha-glucanotransferase HMPREF1322_RS03650
272 (W83: PG0767) and ABC transporter protein gene cluster HMPREF1322_RS00745 (W83: PG1176)
273 and HMPREF1322_RS00740 (W83: PG1175) (Table 6). Seven of the 15 genes had DMAs located
274 upstream of the gene and six of these showed increased 6mA accompanied by decreased gene
275 expression, indicating a potential regulatory effect of 6mA in dampening the expression of *P.*
276 *gingivalis* genes according to hemin availability in the bacterium's microenvironment. Most DMAs
277 annotated to under-expressed genes had higher adenine methylation in excess hemin (84%)
278 regardless of their location with respect to gene structure.

279 One over-expressed and 11 under-expressed genes also had DMCs within 1 kb of the gene (Tables
280 7 and 8). Two of the 11 under-expressed genes had DMCs upstream of the gene (Table 8) with
281 increased methylation levels observed for all 11 genes. Moreover, 95% of DMCs annotated to under-

282 expressed genes had increased cytosine methylation in excess hemin regardless of their location in
283 relation to the gene. This is consistent with results from 6mA, although knowledge of gene
284 regulation by 5mC methylation in bacteria remains limited.

285 Six DEGs had both DMAs and DMCs in their gene body or within ±1kb of the gene (Fig 6), and a
286 subset of these DEGs clustered in a genomic region that includes the lactate utilization gene cluster
287 (Fig 7). The 6 DEGs include the Ppx/GppA family phosphatase HMPREF1322_RS06180 (W83:
288 PG1739), over-expressed in excess hemin, and hypothetical protein HMPREF1322_RS00730 (W83:
289 PG1173), lactate utilization protein HMPREF1322_RS00725 (W83: PG1172), 4-alpha-
290 glucanotransferase HMPREF1322_RS03650 (W83: PG0767), the ABC transporter protein
291 HMPREF1322_RS00745 (W83: PG1176), and HMPREF1322_RS00740 (W83: PG1175), which were
292 under-expressed in excess hemin (Table 9). We assessed whether genome-wide DEGs were
293 enriched for DMAs and DMCs, but did not observe a significant enrichment overall (OR = 0.77 (95%
294 CI: 0.45, 1.31), P-value = 0.38 and OR = 1.13 (95% CI: 0.49, 2.47), P-value = 0.85, respectively).
295 However, we observed strong evidence for overall differences in upstream or gene body DNA
296 methylation levels at specific DEGs overlapping DMAs and DMCs (S5 and S6 Fig).

297 For all DEGs that also harboured DMAs or DMCs, we analysed the overall levels of adenine (S5 Fig)
298 and cytosine (S6 Fig) methylation upstream (−100 bp), downstream (+100 bp) and in the gene body.
299 Differential adenine and cytosine methylation were observed across all regions analysed for the
300 lactate utilization protein HMPREF1322_RS00725 (W83: PG1172) (upstream; gene body;
301 downstream; Table 9; Fig 7). Differential adenine and cytosine methylation were also observed in
302 the gene body of the ABC transporters HMPREF1322_RS00740 (W83: PG1175) and
303 HMPREF1322_RS00745 (W83: PG1176), and hypothetical protein HMPREF1322_RS00730 (W83:
304 PG1173) (S5 and S6 Figs). These ABC transporter proteins are located directly downstream of a
305 lactate utilization gene cluster, which includes the lactate utilization protein and hypothetical
306 protein, possibly highlighting a key region of the *P. gingivalis* genome regulated by DNA methylation
307 (Fig 7). Overall changes in adenine and/or cytosine methylation were also for example observed in
308 the body of the 4−alpha−glucanotransferase HMPREF1322_RS03650 (W83: PG0767) gene, and
309 upstream the ABC transporter HMPREF1322_RS00740 (W83: PG1175) (S5 and S6 Figs).

310

311 Discussion

312 We identified a significant impact of hemin availability in the growth medium on the *P. gingivalis*
313 epigenome and transcriptome. Hemin-dependent differentially modified signatures were identified
314 for gene expression, as well as for 6mA and 5mC methylation profiles. Comparison of the signals
315 highlighted a cluster of coordinated changes in genes related to lactate utilisation and in ABC
316 transporters. The findings identify putative bacterial DNA methylation signatures that may play a
317 regulatory role in the expression of genes, in response to hemin availability.

318 Many of the genes that were over-expressed in excess hemin encoded proteins that contain iron as
319 part of their tertiary structures or iron binding domains in the polyprotein. Furthermore, Lys-
320 gingipain (Kgp; S1 Table) was also over-expressed, and it is involved in iron acquisition and is
321 essential for black pigment (μ-oxo bishaem) formation from hemin and its absence attenuates
322 virulence (11). Members of the ABC transport complex, forming a classical operon, may potentially
323 represent a novel hemin or alternative solute acquisition system that may influence the cellular
324 phenotype. The enhanced expression of thiamine phosphate synthase is not only limited to this gene
325 (S1 Table) of the pathway; the contig also encodes ThiH, ThiG, ThiC, ThiS and a hypothetical

326 protein, all arranged in an apparent operon. Thus, biosynthesis of the energy co-factor thiamine,
327 vitamin B1, constitute an important aspect of *P. gingivalis* metabolism. Rubrerythin offers protection
328 of the anaerobe, *P. gingivalis*, against the toxicity of molecular oxygen and hydrogen peroxide;
329 isogenic mutant is labile under these conditions (22). In addition, there's a preference for
330 succinate/fumarate and α-ketoglutarate utilisation (S1 Table).

331 Many genes under-expressed in excess hemin were involved in hemin binding or transport. Some
332 genes also encoded for DNA transfer functions such as TraC, TraE, TraF and TraJ. Interestingly, the
333 gene encoding the largest protein component of the type IX secretion system (T9SS), Sov (SprA), and
334 also genes encoding OmpH, PorN (GldN) and PorX along with five cargo proteins, are under-
335 expressed in excess hemin (S2 Table). The complex transports over 30 cargo proteins, including
336 known virulence factors, with a C-terminal domain (CTD) signal motif, to the external environment.
337 The surface appendage encoding the long fimbriae, FimA, together with its accessory proteins of the
338 *fim* operon are under-expressed in excess hemin. The genes encoding regulatory proteins (e.g AraC,
339 TetR (AcrR), and LuxR) follow a similar expression pattern. Many transposases were also under-
340 expressed in excess hemin, whereas no transposases were over-expressed in excess hemin,
341 suggesting that the expression of these mobile elements is a characteristic of a stress environment
342 where access to iron is limited.

343 We compared our results with two previous studies exploring expression (23) and proteomic (24)
344 differences in *P. gingivalis* according to hemin availability in the media. We observed that both
345 Anaya-Bergman *et al.* (2015) and Veith *et al.* (2018) previously reported changes in the expression of
346 the phosphomethylpyrimidine synthase ThiC, involved in thiamine biosynthesis, under excess hemin
347 conditions. Moreover, both studies also reported under-expressed levels of the genes coding
348 peroxiredoxin and a phosphotransferase. Separately, Anaya-Bergman et al. (2015) shared three
349 over-expressed genes with our study, *i.e.* the 2-iminoacetate synthase thiH, thiazole synthase thiG
350 and a thiamine phosphate synthase (W83: PG2109/HMPREF1322_RS02110), and Veith et al. (2018)
351 results matched three of the over-expressed genes identified by us, *i.e.* the rubrerythrin family
352 protein HMPREF1322_RS04040 (W83: PG0195) and two hypothetical proteins (W83:
353 PG0717/HMPREF1322_RS01045 and PG2105/HMPREF1322_RS02130). Veith *et. al* (2018) proteomic
354 results also identified proteins for 11 additional under-expressed genes found in our study. These
355 genes coded the cobaltochelatase subunit CobN (W83: PG1553/HMPREF1322_RS06780), the heme-
356 binding protein HmuY(W83: PG1551/HMPREF1322_RS06790), a histidinol phosphate phosphatase
357 (W83: PG0555/HMPREF1322_RS03860), a MMPL family transporter (W83:
358 PG1180/HMPREF1322_RS06005), a peroxiredoxin (W83: PG0618/HMPREF1322_RS06360), a
359 phosphoribosyltransferase (W83: PG1513/HMPREF1322_RS06960), a phosphotransferase (W83:
360 PG0456/HMPREF1322_RS00135), a T9SS type A sorting domain-containing protein (W83:
361 PG0495/HMPREF1322_RS03170), a TonB-dependent receptor (W83:
362 PG1552/HMPREF1322_RS06785), a transporter protein (W83: PG1626/HMPREF1322_RS06460) and
363 three hypothetical proteins (W83: PG0350/HMPREF1322_RS02675, W83:
364 PG0613/HMPREF1322_RS06380, W83: PG1555/HMPREF1322_RS06770). The
365 HMPREF1322_RS06770 hypothetical protein, the HMPREF1322_RS06360 peroxiredoxin and the
366 HMPREF1322_RS06460 transporter respectively matched the PG1555 MotA/TolQ/ExbB proton
367 channel family, PG0618 alkyl peroxide reductase AhpC and PG1626 FADL outer membrane receptor
368 protein annotated in *P. gingivalis* W83 strain genome.

369 Epigenetic mechanisms, including the methylation of specific DNA sequences by DNA
370 methyltransferases, allow unicellular organisms to respond rapidly to environmental stresses (25).

371 Here we showed that both adenines and cytosines can be differentially methylated in *P. gingivalis*
372 according to hemin availability in its microenvironment. Unlike in eukaryotes, in bacteria 5mC is not
373 the dominant DNA modification and instead exists alongside 4mC and 6mA, the latter being the
374 most prevalent modification in prokaryotes (26).Here we characterized both 6mA and 5mC and
375 verified higher levels of adenine methylation ($\bar{x}$ = 23% / $\tilde{x}$ = 13% 6mA genome-wide) in comparison
376 to cytosine methylation ($\bar{x}$ = 18% / $\tilde{x}$ = 13% 5mC genome-wide). However, lack of previous DNA
377 methylation studies in *P. gingivalis* and a general lack of knowledge of the most common genetic
378 motifs targeted by DNA methyltransferases (DNMTs) in this bacterium limited the analyses that we
379 could undertake, and may impact some of the results interpretation. For example, we used
380 Nanopore reads and predictive models in Tombo to estimate the proportion of reads harbouring
381 methylated bases per genomic position in *P. gingivalis*. However, no standard model for methylation
382 calling in *P. gingivalis* exists and therefore we were limited to non-specific all-context methylation
383 calling in our study. This may in turn introduce a higher degree of uncertainty in methylation calling
384 for this bacterium, and we used proportion of methylated reads as an estimate of methylation levels
385 in each sample of bacterial cells. In our data most positions at which DNA methylation was detected
386 were not fully methylated or demethylated, pointing to presence of heterogeneity in the level of
387 DNA methylation across different bacterial cells from the same culture sample (S7 Fig).

388 DNA methylation has historically been associated with bacterial DNA restriction-modification
389 systems, which protect bacterial cells from foreign DNAs (25)]. More recently DNA methylation has
390 also been shown to play important roles in other aspects of bacterial biology such as timing of DNA
391 replication, timing of transposition and conjugal transfer of plasmids, DNA repair and cell
392 partitioning, and regulation of gene expression (25). Less is known however about how widespread
393 the role of DNA methylation is in virulence and pathogenesis. Prior evidence suggests that the
394 activity of DNMTs such as Dam can for example affect virulence in a number of pathogens such as
395 *Escherichia coli, Salmonella* spp., *Yersinia pseudotuberculosis* and *Vibrio cholerae* (27).

396 Here we showed that the availability of hemin – a critical micronutrient that modulates the
397 expression of virulence in *P. gingivalis* – is linked to changes in the DNA methylome of this
398 bacterium. We showed also that methylation changes were coordinated with changes to lactate
399 utilization and ABC transporter genes, however their exact role in *P. gingivalis* remains unknown.
400 Previous research found that lactate utilization (in *Haemophilus influenzae and Staphylococcus*
401 *aureus*) and ABC transport of iron, manganese and/or zinc ions across the membrane (*e.g.,* in
402 *Yersinia pestis, Salmonella enterica* and *Streptococcus* spp.) was linked to an increased virulent
403 status(28-30). In our study, differential methylation in lactate utilization and ABC transporter genes
404 co-occurred with their decreased expression in excess hemin conditions. We hypothesize that the
405 decreased expression of these genes in excess hemin, and conversely their relatively increased
406 expression in limited hemin, could be related to *P. gingivalis* scavenging of nutrients according to
407 their availability in the media.

408 In conclusion, using Nanopore sequencing we were able to characterise for the first time the
409 epigenetic landscape of *P. gingivalis* W50, and to compare epigenetic variation to changes in gene
410 expression. We showed that iron availability in the bacterium's microenvironment can lead to
411 discrete DNA methylation changes potentially impacting the expression of genes related to growth
412 and virulence in humans. There is, however, a need to better characterise the diversity of motifs
413 targeted by different DNMTs, including from *P. gingivalis.* A more comprehensive characterisation of
414 DNMTs and their targeted motifs in the bacterial world will allow better future exploring of DNA
415 methylation in *P. gingivalis* with Oxford Nanopore.

416

417 Materials and Methods

418 Continuous culturing conditions

419 Strain Culture

420 *P. gingivalis* W50 was cultured on Columbia blood agar (CBA; Oxoid) supplemented with 5% oxalated
421 horse blood (Oxoid) incubated anaerobically (5% CO_2/5% H_2/90% N_2) at 37°C for 72 hours. A single
422 colony was inoculated into 100 mL of pre-reduced Brain Heart Infusion (BHI; Oxoid) broth
423 supplemented with 5 mg L^{-1} filter sterilised (0.22 µM) hemin and incubated until late log phase (48-
424 72 hours).

425 Continuous Culture Chemostat Configuration

426 A one litre, sealed glass chemostat was autoclave sterilised with 300 mL BHI *in situ*. 100 mL of *P.*
427 *gingivalis* culture was inoculated into the chemostat through a designated inoculation tube, using a
428 peristaltic pump (Watson Marlow 101U). Sterile BHI (supplemented with either 0.2 or 5 mg L^{-1} hemin
429 for excess and limitation conditions, respectively) was continuously fed at a flow rate of 20 mL h^{-1} to
430 achieve the working volume of 700 mL, before being increased to 70 mL h^{-1}, in conjunction with
431 harvest/waste pump activation at the equivalent rate. Continuous culture represented a dilution
432 rate of 0.1 h^{-1}. Environmental conditions were controlled/monitored using an Applikon ADI 1030 Bio-
433 controller and BioXpert V2 software (Applikon Biotechnology, The Netherlands). The pH of the
434 culture was maintained at pH7±0.1 using 1 M NaOH and 0.5 M HCl fed through a peristaltic pump.
435 Temperature was preserved at 37±0.3°C with a silicon heat jacket. The chemostat was continuously
436 sparged with filter-sterilised 5% CO_2/95% N_2 to maintain anaerobic conditions and stirred at 40 rpm
437 (Motor Controller ADI 1012, Applikon Biotechnology) (S8 Fig).

438 Experimental Design

439 Two independent chemostat experiments were performed, one fed with 5 mg L^{-1} hemin (excess) and
440 one fed with 0.2 mg L^{-1} hemin (limitation). Post-inoculation, the optical density (OD600) of the
441 culture was monitored every 12 hours using a benchtop spectrophotometer (Jenway 6305). Steady
442 state was defined as three consecutive OD600 readings within 10% of each other. Total bacterial
443 populations were enumerated daily in a Whitley A45 anaerobic Workstation (Don Whitley Scientific,
444 UK), through a serial dilution (in phosphate buffered saline; PBS) and triplicate plating method on
445 CBA. Purity of the culture was visually assessed from these agars. Sampling for DNA and RNA analysis
446 was performed every 48 hours during steady state (Fig 1). This represented biological replicates
447 separated by five full volume replenishments of the chemostat vessel.

448 Nucleic Acid Sampling

449 During nucleic acid sampling periods the harvest bottle was replaced with a sterile collection bottle
450 (on ice) and approximately 20 mL was collected. For DNA sampling, 1 mL aliquots were centrifuged
451 at 13,000 rpm for 10 minutes (4°C), prior to supernatant removal and storage at −80°C. For RNA
452 samples, ten 1 mL samples were centrifuged as previously described, the supernatant decanted, and
453 the pellet reconstituted in 1mL of DNA/RNA Shield (Zymo Research, USA), prior to storage at −80°C.

454 DNA extraction

455 One mL cultures were centrifuged at 17,000×g, at 4°C for 10 minutes. The pellets were used to
456 extract high molecular weight DNA using Gentra Puregene yeast/bacteria DNA isolation kit (Qiagen),
457 following the manufacturer's protocol. DNA was finally resuspended in 200 µl EB buffer (Qiagen) and
458 stored at 4°C before use.

459 ## RNA extraction

460 Cells were pelleted as above and resuspended/lysed in 350 µl of DNA/RNA Shield (Cambridge
461 Biosciences) at room temperature. The solutions were used directly in RNA isolation with Zymo
462 Quick-RNA™ miniprep kit (Cambridge Biosciences) in accordance with the manufacture's protocol.
463 This incorporated the initial chromosomal DNA removal, and on-column DNAase I digestion before
464 the final wash and elution into 50 µl nuclease-free water. RNA was stored at −70°C.

465 ## Illumina RNA sequencing

466 RNA samples were first subjected to rRNA depletion using the NEBNext® rRNA Depletion Kit
467 (Bacteria). The samples were then used for RNA-seq library preparation using the NEBNext Ultra II
468 Directional RNA Library Prep Kit for Illumina. Both kits were used according to the manufacturer's
469 instructions. Sequencing was performed by Novagene, UK on an Illumina Novaseq6000 instrument.

470 ## Oxford Nanopore DNA sequencing

471 MinIon library preparation and DNA sequencing was performed at the University of Nottingham on
472 MinIon flow cell (Oxford Nanopore). Whole-genome sequencing libraries were prepared from six
473 bacterial genomic DNA samples. DNA samples were quantified using the Qubit 4 Fluorometer
474 (Thermo Fisher Scientific) and the Qubit dsDNA BR Assay Kit (Thermo Fisher Scientific; Q32853) and
475 the Agilent 4200 TapeStation and the Agilent Genomic DNA ScreenTape Assay (Agilent; 5067-5365
476 and 5067-5366) were used to assess the molecular weight of the DNA. Sequencing libraries were
477 prepared using the Native barcoding genomic DNA protocol (Oxford Nanopore Technologies;
478 Version: NBE_9065_v109_revS_14Aug2019). This protocol uses the Ligation Sequencing Kit (Oxford
479 Nanopore Technologies; SQK-LSK109) and the Native Barcoding Expansion 1-12 kit (Oxford
480 Nanopore Technologies; EXP-NBD104) to barcode the unsheared DNA fragments within each
481 sample. Barcoded samples were then pooled in equimolar amounts for the final sequencing adapter
482 ligation. All purification steps were performed using AMPure XP beads (Beckman Coulter; A63882).
483 The final barcoded library pool was loaded onto a MinION flow cell (Oxford Nanopore Technologies;
484 FLO-MIN106 R9.4.1) and run on the GridION X5 Mk1.

485 ## Bioinformatic analysis

486 ### RNA sequencing data processing

487 Sequencing data was processed using the ProkSeq pipeline(18) Briefly, FastQC (31)and AfterQC (32,
488 33) were implemented to check the quality of data, trim adaptor sequences and filter out low quality
489 reads using standard parameters. This resulted in a total of ≈25.3–36.0 M PE reads (2 × 76 bp) being
490 kept for downstream processing. Subsequently, bowtie2 (32) was used to align reads against the
491 104 contigs of the *P. ginigivalis* W50 genome assembly deposited in the NCBI RefSeq (accession no.
492 GCF_000271945.1). RefSeq gene annotations were extracted from *P. ginigivalis*' GTF file and the
493 number of total reads per gene were calculated using featureCounts (34)]. Counts per gene were
494 estimated for 1992 genes. RSeQC (35) was used to study sample coverage uniformity along the body
495 of genes.

496 ### DNA methylation calling

497 Total Nanopore read data included ≈240–380 K reads (88 bp – 143 kb, N50 = 27 kb) per sample.
498 Nanopore signals were originally stored in multi read fast5 files and the *ont_fast5_api*
499 'multi_to_single_fast5' (47) was used to generate single fast5 files before detection of non-standard
500 nucleotides with Tombo (36). First, electric current signal level data was re-squiggled using the same
501 *P. ginigivalis* W50 reference genome used to pre-process the RNA-Seq data. Secondly, all-context
502 motif-independent models were used in Tombo to detect the alternative bases 6mA and 5mC from

503 the signal data. Alternative base calling in each sample was summarized per genomic position with
504 coverage and dampened fractions estimated at each adenine and cytosine site of both positive and
505 negative DNA strands. Coverage was stored in the bedGraph format and proportion of methylation
506 in the WIG format. Data files were imported into R using the package *rtracklayer* (37) and combined
507 into a single data frame using GRanges, IRanges and *findOverlaps* from the IRanges package (38)

508 The proportion of methylation – dampened fraction – was estimated by adjusting the proportion of
509 methylated reads according to coverage at low coverage sites in order to include them in
510 downstream analyses (36). Despite this, only adenines and cytosines with at least 10× coverage
511 across samples were included in our analysis. Overall, 1,150,659 adenines and 1,079,809 cytosines
512 were kept for downstream analyses, with 350–525× mean base coverage per sample.

513 Statistical analyses

514 Differential gene expression analysis

515 DESeq2 (19) was used to normalize the read count data and perform differential gene expression
516 analysis. Growth in limited hemin was the 'control' and growth in excess hemin was the 'treatment'.
517 All three samples from each condition were used and global sample differences were observed using
518 the principal component analysis method. Both DESeq2 and edgeR (39) were implemented from
519 ProkSeq's downstream analysis. Both methods allow for inter-sample comparison in differential
520 gene expression analysis. Here we used edgeR results as sensitivity for DESeq2 results since edgeR
521 normalizes expression data differently to DESeq2 (DESeq2 uses the median of ratios method and
522 edgeR uses the trimmed mean of M values to normalize read count data). The false discovery rate
523 method (FDR) was used to identify differentially expressed genes and genes with FDR < 5% and a
524 $\log_2$ fold change (LFC) > 1.5 or < −1.5 were respectively considered over and under-expressed in
525 excess hemin. Differentially expressed genes were subsequently manually annotated to the *P.*
526 *gingivalis* W83 genome (GenBank accession no. AE015924) (21) in order to compare results with
527 previous research. Synteny analysis at specific loci was performed using MAUVE (40).

528 Gene ontology enrichment analysis

529 Gene ontology (GO) enrichment analysis in over and under-expressed gene sets was performed
530 using ShinyGO (41). Because *P. gingivalis* W50's genome was not available from ShinyGO's species
531 database, only well-characterized genes that matched gene symbols in *P. gingivalis* W83 reference
532 strain genome were used in this analysis. A more relaxed FDR threshold of 10% was applied to assess
533 enrichment in this case and GO molecular functions were reported.

534 Differential DNA methylation analysis

535 Mean and median DNA methylation across samples were calculated using all adenines and cytosines
536 kept for downstream analysis. Global DNA methylation differences between the samples were
537 observed using principal component analysis for 6mA and 5mC modifications, selecting for minimum
538 10× and 100× coverage per position.

539 Two-sided Student's t-tests were applied at each adenine and cytosine site after filtering for
540 positions where was at least a 5% mean methylation difference was observed between the
541 experimental conditions (139,794 adenines and 87,398 cytosines). A sensitivity analysis was
542 performed for minimum 100× coverage (85,090 adenines and 46,930 cytosines) to ascertain
543 whether the significance of results was impacted by depth of sequencing. Results were considered
544 statistically significant at an FDR threshold of 5% to match gene expression analysis.

545 The differentially methylated positions identified were annotated to nearby genes considering the
546 location and gene strand. First, DMAs and DMCs were annotated to the gene if they were located in
547 a gene body, and second, DMAs and DMCs were annotated to genes found in the same contig and
548 within ±1kb of their location. Genes located in the opposite strand of the methylation signal were
549 considered in both cases.

550 In comparing the overlap between DEGs, DMA, and DMCs, we considered all DMAs and DMCs that
551 were in or near the gene (±1 kb away, both strands). This data was also used to explore DNA
552 methylation effects on the expression of nearby genes. A contingency table containing all 1192
553 genes was constructed and Fischer's exact tests were employed to test for the enrichment of genes
554 with concurrent gene expression and DNA methylation changes. The enrichment of differential DNA
555 methylation directly upstream, downstream and in the body of genes was also tested. Here,
556 Wilcoxon signed-rank tests were used to test for generalized shifts in DNA methylation signals
557 between the experimental conditions 100 bp upstream, 100 bp downstream and within the body of
558 genes previously annotated to DMAs and/or DMCs.

559 Motif enrichment analysis

560 The MEME (Multiple EM for Motif Elicitation) online tool (42)was used to detect enriched motifs
561 containing the DMAs and DMCs identified with concurrent gene expression changes. For this, 15
562 base pair long DNA sequences surrounding the DMAs and DMCs identified were extracted.
563 Subsequently, motifs with minimum 4 bp and maximum 15 bp were searched using MEME's Classic
564 objective function and the ZOOPS distribution model. Both the given strand and the reverse
565 complement strand were considered, and the top 10 motifs found were reported. Motifs were
566 considered significant if their reported E-value threshold was ≤ 0.05.

567

568 Acknowledgments

569 We are grateful to the Medical Research Council of United Kingdom for the grant: MR/P012175/2.
570 We thank Mr Darioush Yarand and the Rosalind KCL high performance linux cluster system
571 administration team for help resolving file space and software installation queries.

572

573 References

574 1. Curtis MA, Zenobia C, Darveau RP. The relationship of the oral microbiotia to periodontal
575 health and disease. Cell Host Microbe. 2011;10(4):302-6.
576 2. Curtis MA, Diaz PI, Van Dyke TE. The role of the microbiota in periodontal disease.
577 Periodontol 2000. 2020;83(1):14-25.
578 3. Dominy SS, Lynch C, Ermini F, Benedyk M, Marczyk A, Konradi A, et al. in Alzheimer's disease
579 brains: Evidence for disease causation and treatment with small-molecule inhibitors. Sci Adv.
580 2019;5(1):eaau3333.
581 4. Sedghi LM, Bacino M, Kapila YL. Periodontal Disease: The Good, The Bad, and The Unknown.
582 Front Cell Infect Microbiol. 2021;11:766944.
583 5. Holt SC, Ebersole JL. *Porphyromonas gingivalis*, *Treponema denticola*, and *Tannerella*
584 *forsythia*: the "red complex", a prototype polybacterial pathogenic consortium in periodontitis.
585 Periodontol 2000. 2005;38:72-122.

586 6. Hajishengallis G, Liang S, Payne MA, Hashim A, Jotwani R, Eskan MA, et al. Low-abundance
587 biofilm species orchestrates inflammatory periodontal disease through the commensal microbiota
588 and complement. Cell Host Microbe. 2011;10(5):497-506.
589 7. Payne MA, Hashim A, Alsam A, Joseph S, Aduse-Opoku J, Wade WG, et al. Horizontal and
590 Vertical Transfer of Oral Microbial Dysbiosis and Periodontal Disease. J Dent Res. 2019;98(13):1503-
591 10.
592 8. Smalley JW, Thomas MF, Birss AJ, Withnall R, Silver J. A combination of both arginine- and
593 lysine-specific gingipain activity of *Porphyromonas gingivalis* is necessary for the generation of the
594 micro-oxo bishaem-containing pigment from haemoglobin. Biochem J. 2004;379(Pt 3):833-40.
595 9. Lamont RJ, Jenkinson HF. Life below the gum line: pathogenic mechanisms of
596 *Porphyromonas gingivalis*. Microbiol Mol Biol Rev. 1998;62(4):1244-63.
597 10. Lunar Silva I, Cascales E. Molecular Strategies Underlying *Porphyromonas gingivalis*
598 Virulence. J Mol Biol. 2021;433(7):166836.
599 11. Curtis MA, Aduse Opoku J, Rangarajan M, Gallagher A, Sterne JA, Reid CR, et al. Attenuation
600 of the virulence of *Porphyromonas gingivalis* by using a specific synthetic Kgp protease inhibitor.
601 Infect Immun. 2002;70(12):6968-75.
602 12. Smalley JW, Olczak T. Heme acquisition mechanisms of *Porphyromonas gingivalis* - strategies
603 used in a polymicrobial community in a heme-limited host environment. Mol Oral Microbiol.
604 2017;32(1):1-23.
605 13. Mattos-Graner RO, Duncan MJ. Two-component signal transduction systems in oral bacteria.
606 J Oral Microbiol. 2017;9(1):1400858.
607 14. Jiang C, Yang D, Hua T, Hua Z, Kong W, Shi Y. A PorX/PorY and σ^P Feedforward
608 RegulatoryLoop Controls Gene Expression Essential for *Porphyromonas gingivalis* Virulence.
609 mSphere. 2021;6(3):e0042821.
610 15. Yang D, Jiang C, Ning B, Kong W, Shi Y. The PorX/PorY system is a virulence factor of
611 Porphyromonas gingivalis and mediates the activation of the type IX secretion system. J Biol Chem.
612 2021;296:100574.
613 16. Murphy TR, Xiao R, Hamilton-Brehm SD. Hybrid genome de novo assembly with methylome
614 analysis of the anaerobic thermophilic subsurface bacterium *Thermanaerosceptrum fracticalcis*
615 strain DRI-13T. BMC Genomics. 2021;22(1):209.
616 17. Tourancheau A, Mead EA, Zhang XS, Fang G. Discovering multiple types of DNA methylation
617 from bacteria and microbiome using nanopore sequencing. Nat Methods. 2021;18(5):491-8.
618 18. Firoj Mahmud AKM, Delhomme N, Nandi S, Fällman M. ProkSeq for complete analysis of
619 RNA-Seq data from prokaryotes. Bioinformatics. 2020.
620 19. Love MI, Huber W, Anders S. Moderated estimation of fold change and dispersion for RNA-
621 seq data with DESeq2. Genome Biol. 2014;15(12):550.
622 20. Kondo Y, Ohara N, Sato K, Yoshimura M, Yukitake H, Naito M, et al. Tetratricopeptide repeat
623 protein-associated proteins contribute to the virulence of *Porphyromonas gingivalis*. Infect Immun.
624 2010;78(6):2846-56.
625 21. Nelson KE, Fleischmann RD, DeBoy RT, Paulsen IT, Fouts DE, Eisen JA, et al. Complete
626 genome sequence of the oral pathogenic Bacterium *Porphyromonas gingivalis* strain W83. J
627 Bacteriol. 2003;185(18):5591-601.
628 22. Sztukowska M, Bugno M, Potempa J, Travis J, Kurtz DM. Role of rubrerythrin in the oxidative
629 stress response of *Porphyromonas gingivalis*. Mol Microbiol. 2002;44(2):479-88.
630 23. Anaya-Bergman C, Rosato A, Lewis JP. Iron- and hemin-dependent gene expression of
631 *Porphyromonas gingivalis*. Mol Oral Microbiol. 2015;30(1):39-61.
632 24. Veith PD, Luong C, Tan KH, Dashper SG, Reynolds EC. Outer Membrane Vesicle Proteome of
633 *Porphyromonas gingivalis* Is Differentially Modulated Relative to the Outer Membrane in Response
634 to Heme Availability. J Proteome Res. 2018;17(7):2377-89.
635 25. Casadesús J, Low D. Epigenetic gene regulation in the bacterial world. Microbiol Mol Biol
636 Rev. 2006;70(3):830-56.

637 26. Beaulaurier J, Schadt EE, Fang G. Deciphering bacterial epigenomes using modern
638 sequencing technologies. Nat Rev Genet. 2019;20(3):157-72.
639 27. Low DA, Weyand NJ, Mahan MJ. Roles of DNA adenine methylation in regulating bacterial
640 gene expression and virulence. Infect Immun. 2001;69(12):7197-204.
641 28. Garmory HS, Titball RW. ATP-binding cassette transporters are targets for the development
642 of antibacterial vaccines and therapies. Infect Immun. 2004;72(12):6757-63.
643 29. Fuller JR, Vitko NP, Perkowski EF, Scott E, Khatri D, Spontak JS, et al. Identification of a
644 lactate-quinone oxidoreductase in Staphylococcus aureus that is essential for virulence. Front Cell
645 Infect Microbiol. 2011;1:19.
646 30. Lichtenegger S, Bina I, Roier S, Bauernfeind S, Keidel K, Schild S, et al. Characterization of
647 lactate utilization and its implication on the physiology of *Haemophilus influenzae*. Int J Med
648 Microbiol. 2014;304(3-4):490-8.
649 31. Wingett SW, Andrews S. FastQ Screen: A tool for multi-genome mapping and quality control.
650 F1000Res. 2018;7:1338.
651 32. Langmead B, Salzberg SL. Fast gapped-read alignment with Bowtie 2. Nat Methods.
652 2012;9(4):357-9.
653 33. Chen S, Huang T, Zhou Y, Han Y, Xu M, Gu J. AfterQC: automatic filtering, trimming, error
654 removing and quality control for fastq data. BMC Bioinformatics. 2017;18(Suppl 3):80.
655 34. Liao Y, Smyth GK, Shi W. featureCounts: an efficient general purpose program for assigning
656 sequence reads to genomic features. Bioinformatics. 2014;30(7):923-30.
657 35. Wang L, Wang S, Li W. RSeQC: quality control of RNA-seq experiments. Bioinformatics.
658 2012;28(16):2184-5.
659 36. Stoiber M, Quick J, Egan R, Eun Lee J, Celniker S, Neely RK, et al. *De novo* Identification of
660 DNA Modifications Enabled by Genome-Guided Nanopore Signal Processing. bioRxiv. 2022:094672.
661 37. Lawrence M, Gentleman R, Carey V. rtracklayer: an R package for interfacing with genome
662 browsers. Bioinformatics. 2009;25(14):1841-2.
663 38. Lawrence M, Huber W, Pagès H, Aboyoun P, Carlson M, Gentleman R, et al. Software for
664 computing and annotating genomic ranges. PLoS Comput Biol. 2013;9(8):e1003118.
665 39. Robinson MD, McCarthy DJ, Smyth GK. edgeR: a Bioconductor package for differential
666 expression analysis of digital gene expression data. Bioinformatics. 2010;26(1):139-40.
667 40. Darling AE, Mau B, Perna NT. progressiveMauve: multiple genome alignment with gene gain,
668 loss and rearrangement. PLoS One. 2010;5(6):e11147.
669 41. Ge SX, Jung D, Yao R. ShinyGO: a graphical gene-set enrichment tool for animals and plants.
670 Bioinformatics. 2020;36(8):2628-9.
671 42. Bailey TL, Williams N, Misleh C, Li WW. MEME: discovering and analyzing DNA and protein
672 sequence motifs. Nucleic Acids Res. 2006;34(Web Server issue):W369-73.

673 43. Hajishengallis G. Interconnection of periodontal disease and comorbidities: Evidence,
674 mechanisms, and implications. Periodontol 2000; 00: 1– 10.

675 44. Hajishengallis G, Liang S, Payne MA, Hashim A, Jotwani R, Eskan MA, McIntosh ML, Alsam A,
676 Kirkwood KL, Lambris JD, Darveau RP, Curtis MA. Low-abundance biofilm species orchestrates
677 inflammatory periodontal disease through the commensal microbiota and complement. Cell Host
678 Microbe. 2011 Nov 17;10(5):497-506.

679 45. Payne MA, Hashim A, Alsam A, Joseph S, Aduse-Opoku J, Wade WG, Curtis MA. Horizontal
680 and Vertical Transfer of Oral Microbial Dysbiosis and Periodontal Disease. J Dent Res. 2019
681 Dec;98(13):1503-1510.

682 46. Haurat MF, Aduse-Opoku J, Rangarajan M, Dorobantu L, Gray MR, Curtis MA, Feldman MF.
683 Selective sorting of cargo proteins into bacterial membrane vesicles. J Biol Chem. 2011 Jan
684 14;286(2):1269-76.

685 47. Sato K, Naito M, Yukitake H, Hirakawa H, Shoji M, McBride MJ, Rhodes RG, Nakayama K. A
686 protein secretion system linked to bacteroidete gliding motility and pathogenesis. Proc Natl Acad Sci
687 U S A. 2010 Jan 5;107(1):276-81.

688 48. ont_fast5_api. Available at: https://github.com/nanoporetech/ont_fast5_api

689

690 Supporting information

691 **S1 Fig.** Overlap between DeSeq2 and edgeR results for differentially expressed *P. gingivalis* genes
692 cultured in excess hemin conditions.

693 **S2 Fig.** DESeq2-normalized counts PCA for *P. gingivalis* growth in limited (red) and excess (blue)
694 hemin conditions.

695 **S3 Fig.** DNA methylation PCA for *P. gingivalis* growth in limited (LiH) and excess (ExH) hemin
696 conditions, selecting for 10× (A) and 100× (B) coverage.

697 **S4 Fig.** MEME motif analysis results for the 49 and 47 DMAs and DMCs identified in the main
698 analysis.15-nucleotide long sequences surrounding DMAs and DMCs were extracted, and motifs
699 were analysed considering minimum and maximum motif widths of 4 and 15 nucleotides,
700 respectively. A maximum number of 10 motifs were searched. No motifs reached significance (E-
701 value < 0.05).

702 **S5 Fig.** Adenine methylation patterns upstream (−100 bp), downstream (+100 bp) and in the gene
703 body of differentially expressed genes annotated to DMAs. Differential methylation significance was
704 tested using Wilcoxon signed-rank tests between limited (red) and excess (blue) hemin conditions.

705 **S6 Fig.** Cytosine methylation patterns upstream (−100 bp), downstream (+100 bp) and in the gene
706 body of differentially expressed genes annotated to DMAs. Differential methylation significance was
707 tested using Wilcoxon signed-rank tests between limited (red) and excess (blue) hemin conditions.

708 **S7 Fig.** Distribution of DNA methylation for *P. gingivalis* growth in limited (LiH) and excess (ExH)
709 hemin conditions, selecting for 10× (A) and 100× (B) coverage.

710 **S8 Fig.** Schematic representation of chemostat set up in class II fume cabinet.

711 **S1 Table.** Genes over-expressed in excess hemin conditions (>1.5 LFC, FDR = 5%).

712 **S2 Table.** Genes under-expressed in excess hemin conditions (<−1.5 LFC, FDR = 5%).

713 **S3 Table.** GO molecular functions over-expressed in excess hemin conditions (based on 40 genes,
714 FDR = 10%).

715 **S3 Table.** GO molecular functions under-expressed in excess hemin conditions (based on 8 genes,
716 FDR = 10%).

717 **S5 Table.** DMAs (6mA) identified in *P. gingivalis* W50, selecting for minimum 100× coverage and
718 mean 5% methylation difference between experimental conditions (FDR = 5%).

719 **S6 Table.** DMCs (5mC) identified in *P. gingivalis* W50, selecting for minimum 100× coverage and
720 mean 5% methylation difference between experimental conditions (FDR = 5%).

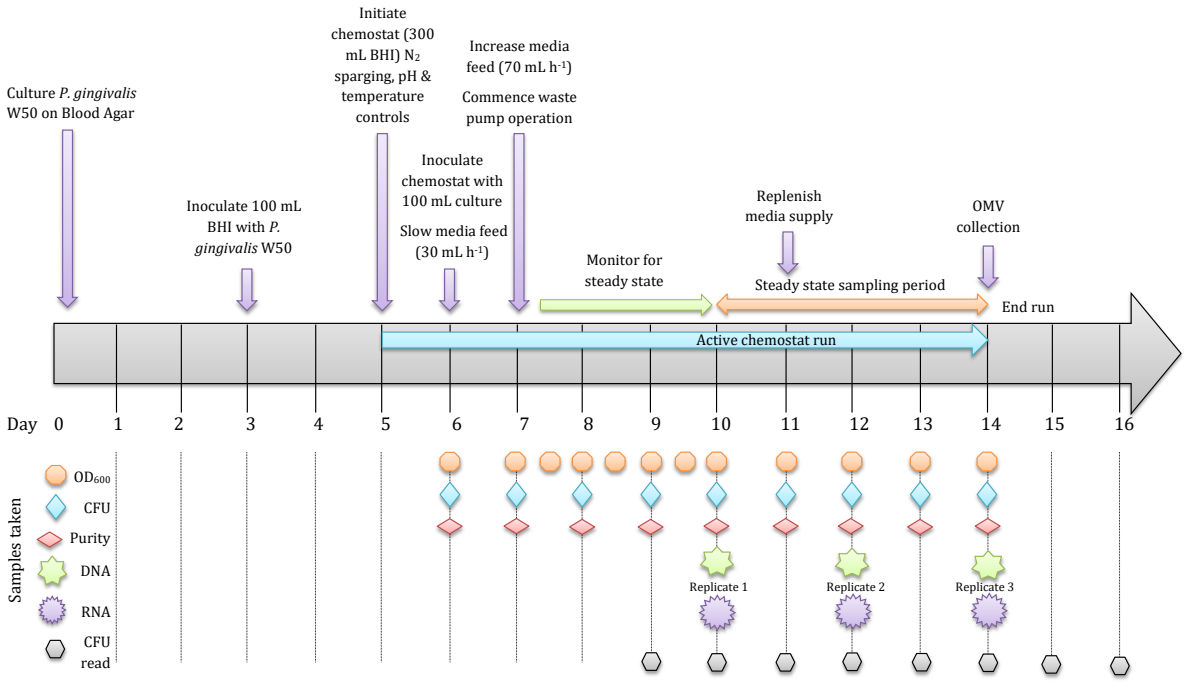

Fig 1. Timeline of *P. gingivalis* W50 chemostat operation and experimental design. CFU – colony forming unit, BHI – Brain Heart Infusion.

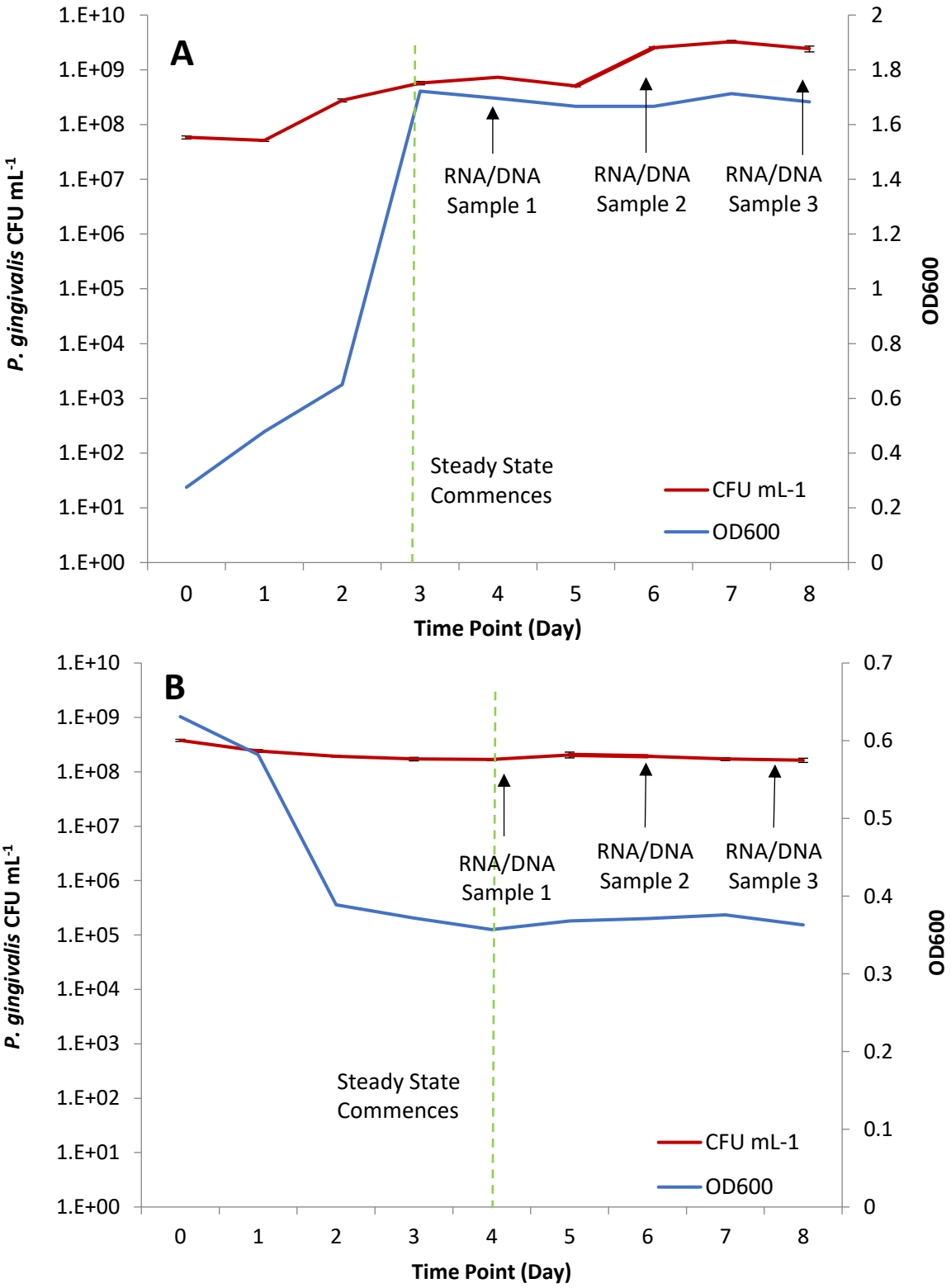

Fig 2. Enumeration of *P. gingivalis* populations throughout the continuous culture chemostat experimental duration by colony count and optical density (OD). A – *P. gingivalis* W50 cultured with excess hemin (5 mg L^{-1}). B – *P. gingivalis* W50 cultured with limited hemin (0.2 mg L^{-1}). CFU – colony forming units. Error bars represent standard error of the mean.

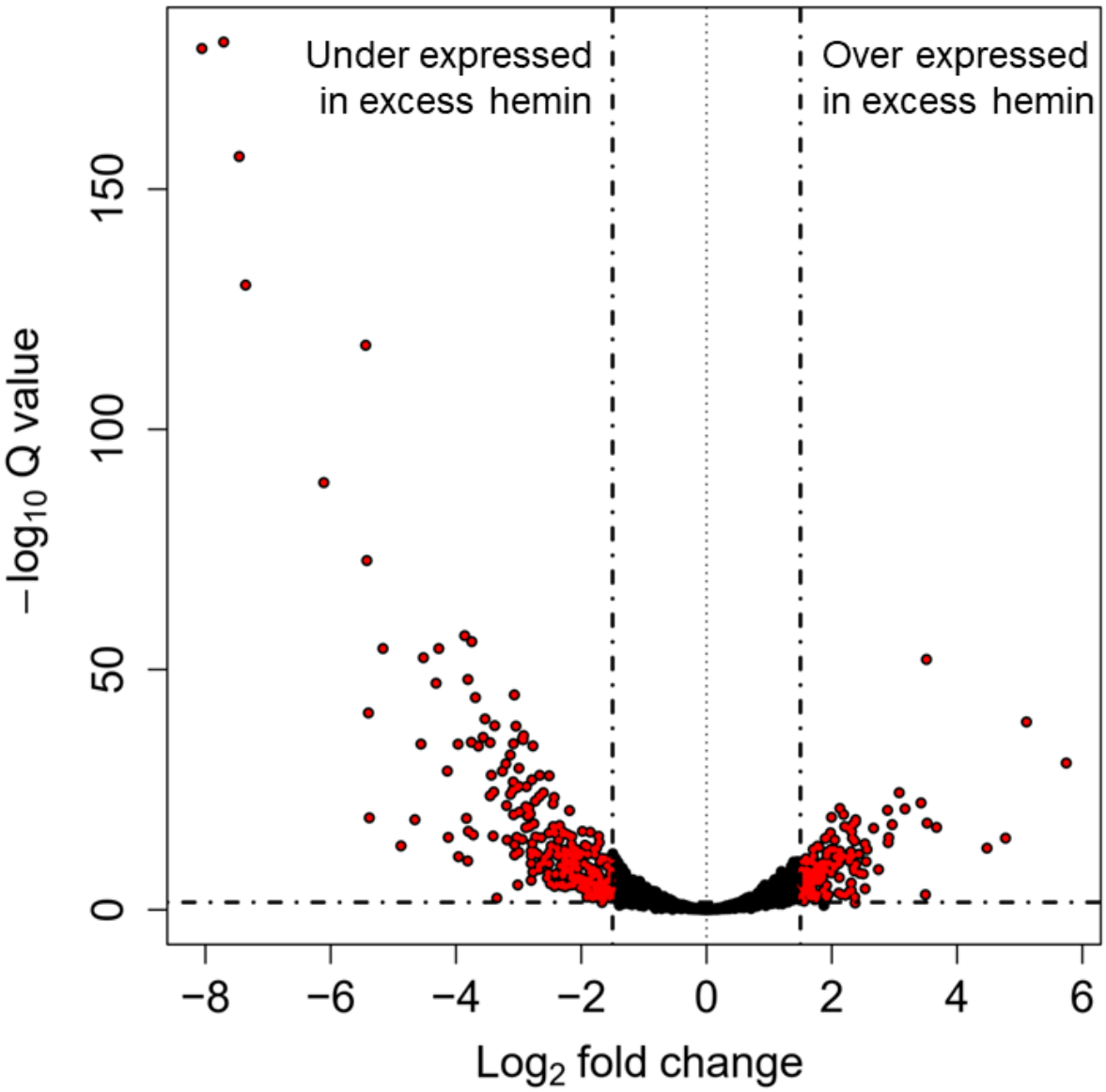

Fig 3. Differentially expressed genes in excess hemin conditions. *P. gingivalis* genes were considered differentially expressed if transcript abundance surpassed 1.5 LFC between culturing conditions (FDR = 5%).

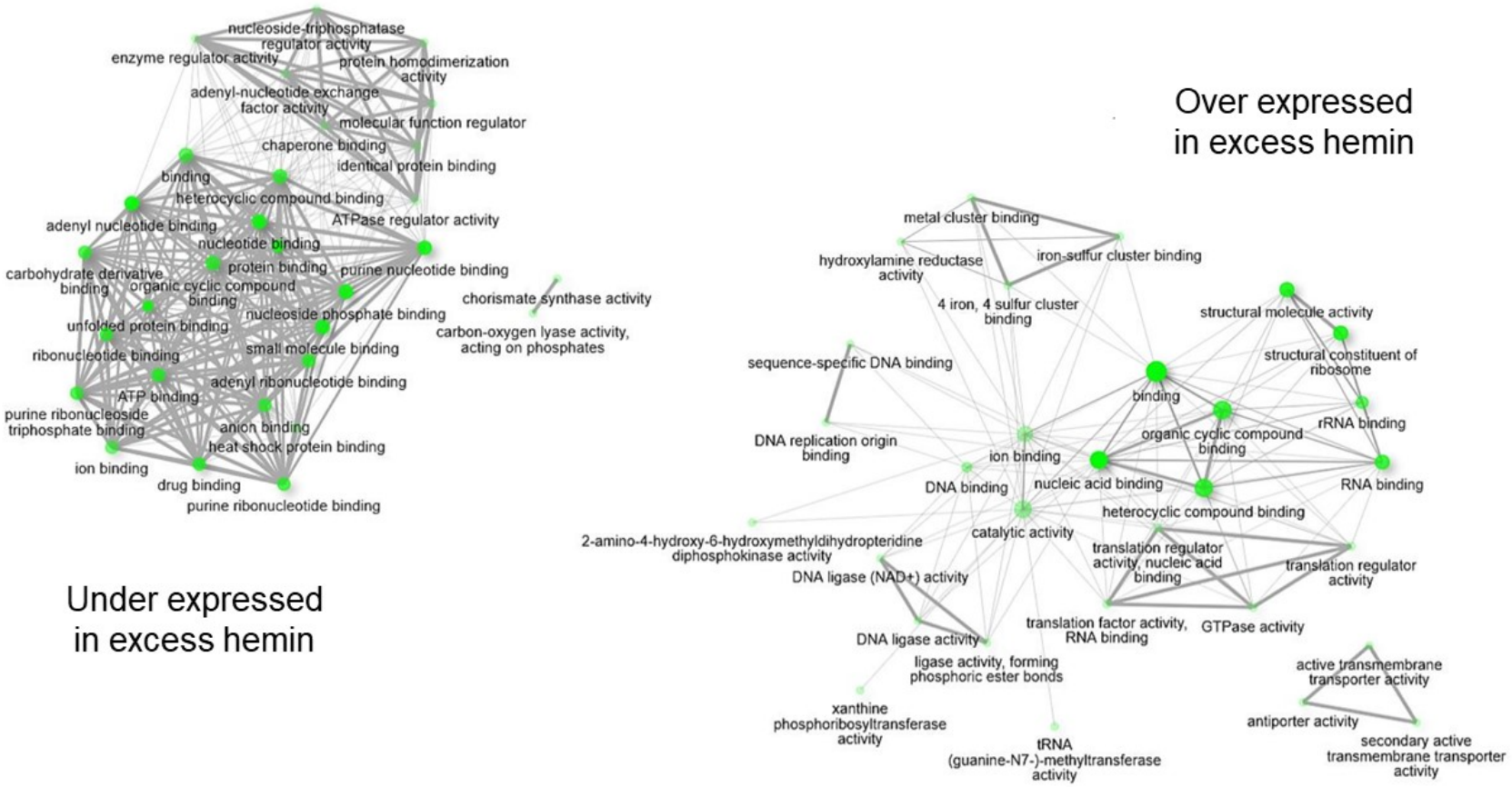

Fig 4. GO molecular function enrichment of genes under and over-expressed in excess hemin conditions (1.5 LFC, FDR = 10%). The top 30 GO molecular functions were selected to create the networks and edges represent pathways with > 10% shared genes. Darker nodes are more significantly enriched, bigger nodes represent larger gene sets and thicker edges correspond to more overlaps between gene sets. Pathways were created based on gene matches to *P. gingivalis* W83 reference genome.

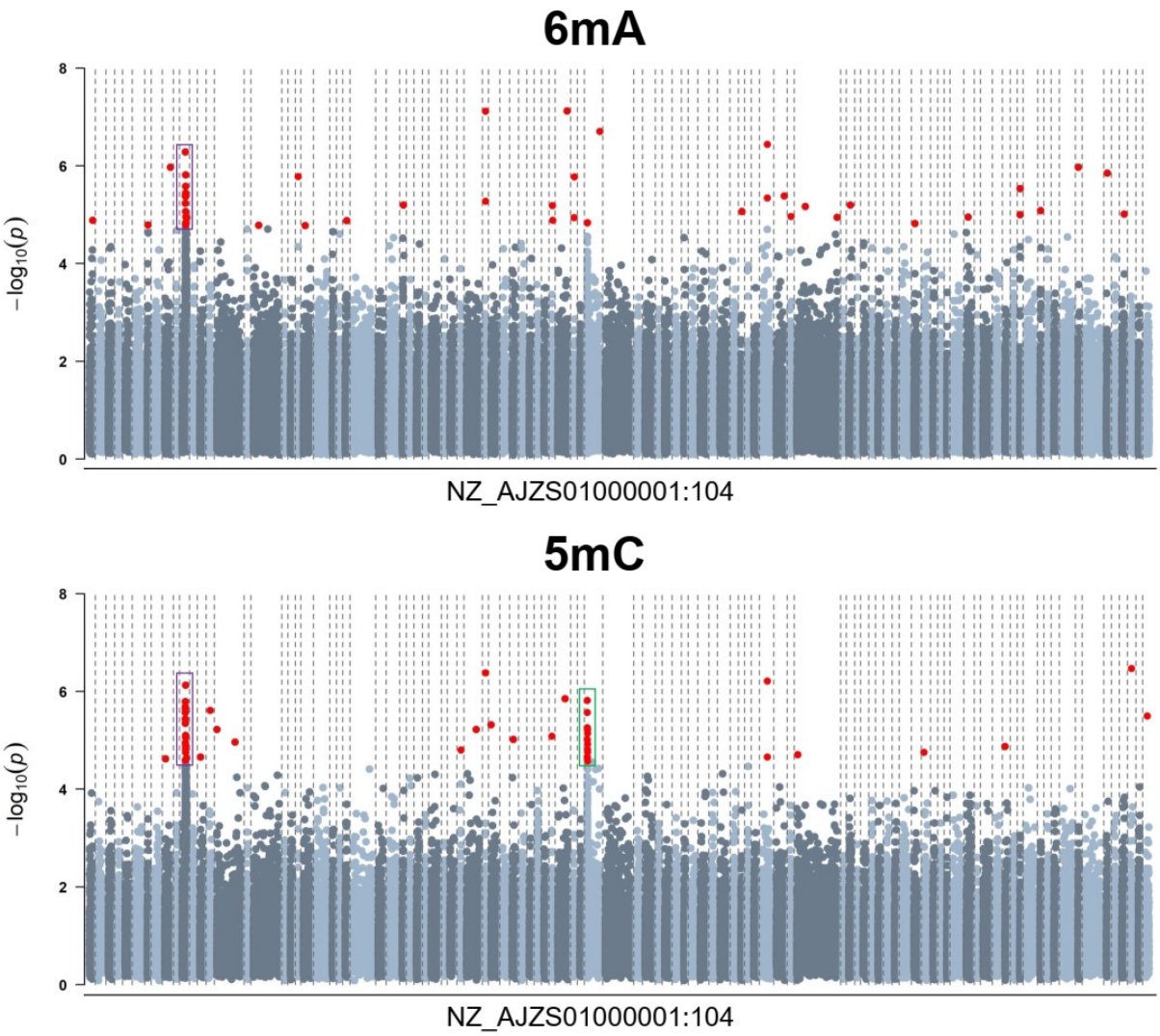

Fig 5. Differential methylation analysis results for excess hemin. Results are presented for 139,794 adenines (6mA) and 87,398 cytosines (5mC) showing a minimum 5% mean methylation difference between experimental conditions. Contigs were plotted in ascending order (NZ_AJZS01000001:104) and delimited by dashed lines in the graph. Genomic positions surpassing the FDR = 5% significance threshold are depicted in red. Clusters of DMAs and DMCs are highlighted in purple and green. The DMA/DMC cluster highlighted in purple is shown in detail in Fig 7.

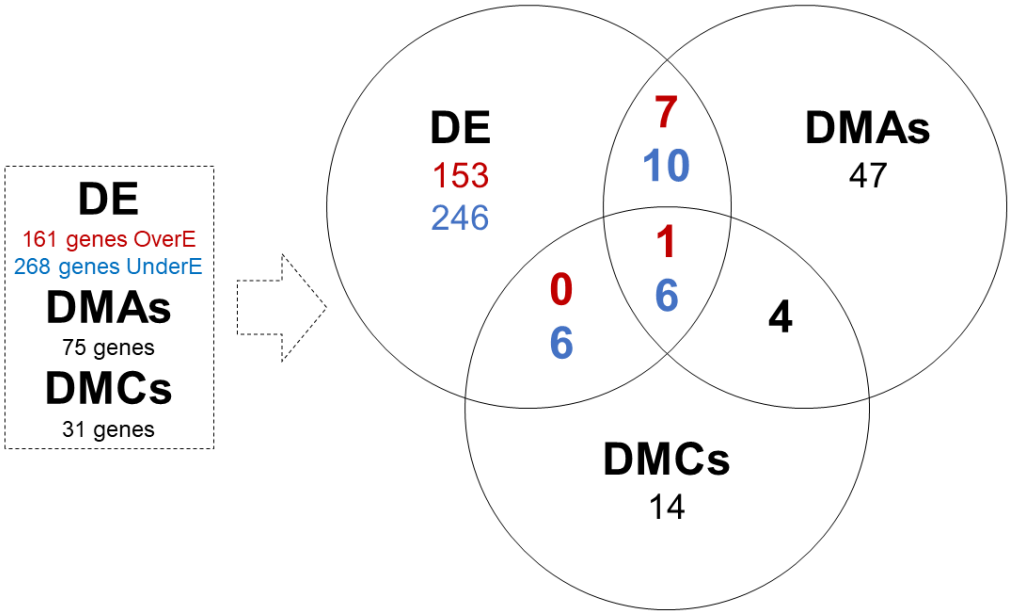

Fig 6. Overlap of genes with differential gene expression (DE), DMAs and DMCs in excess hemin conditions.

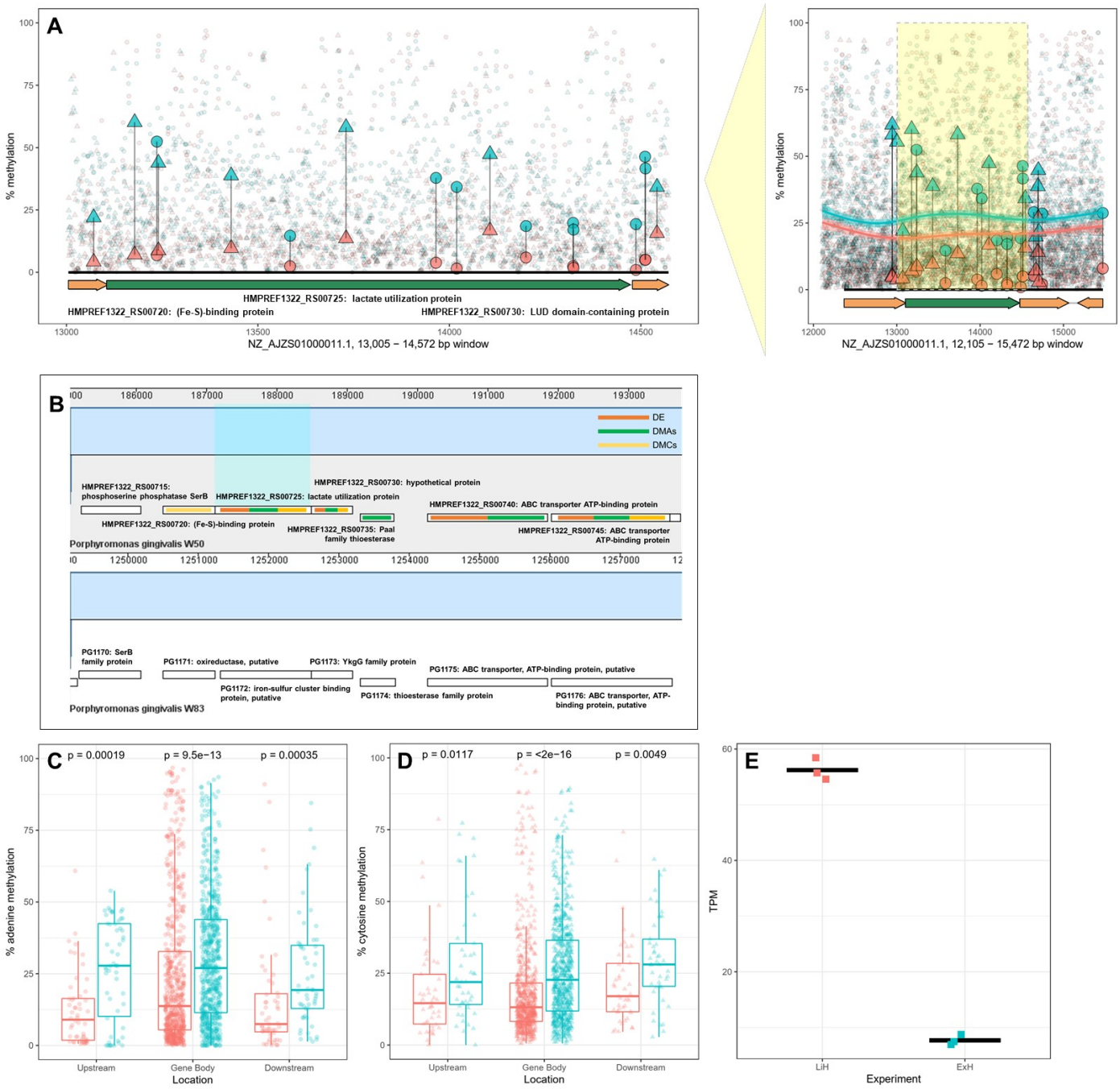

Fig 7. Genomic cluster of differential expression, adenine and cytosine methylation in the lactate utilization protein (HMPREF1322_RS00725) gene locus. Adenine (circles) and cytosine (triangles) percentage of methylation in this gene locus are shown in limited (LiH; red) and excess (ExH; blue) hemin conditions. DMAs and DMCs (larger data points) were observed within a 100 bp or 1000 bp window from the gene and a generalized additive model curve was fitted to the methylation values (A). The lactate utilization protein HMPREF1322_RS00725 was located in a cluster of genes conserved between *P. gingivalis* W50 and reference strain W83 (B). Genes in this location were affected by both DNA methylation (DMA/DMC) and gene expression (DE) changes. Differential adenine (C) and cytosine (D) methylation was statistically significant upstream (−100 bp), downstream (+100 bp) and in the gene body of HMPREF1322_RS00725 using the Wilcoxon signed-ranked test. Increased methylation in ExH was accompanied by decreased gene expression of HMPREF1322_RS00725 (E).

Table 1. Genes most over-expressed in excess hemin conditions ordered by their significance P-value. The complete list of 161 genes is included in S1 Table.

Locus Tag	baseMean	LFC	lfcSE	P-value	Gene Symbol	Gene Product
HMPREF1322_RS04040	36595.19	3.51	0.22	5.16E-55	-	rubrerythrin family protein
HMPREF1322_RS09700	10401.67	5.11	0.38	7.99E-42	-	4Fe-4S dicluster domain-containing protein
HMPREF1322_RS02110	21476.06	5.74	0.48	4.96E-33	-	thiamine phosphate synthase
HMPREF1322_RS04875	4568.08	3.08	0.29	1.10E-26	-	RnfABCDGE type electron transport complex subunit G
HMPREF1322_RS09380	6878.27	3.42	0.34	1.63E-24	-	tRNA-Ala
HMPREF1322_RS01360	88636.17	2.13	0.21	2.51E-23	-	Lys-gingipain
HMPREF1322_RS07500	8156.19	3.17	0.32	3.27E-23	-	FtsX-like permease family protein
HMPREF1322_RS04865	8535.61	2.89	0.29	6.34E-23	*rsxC*	electron transport complex subunit RsxC
HMPREF1322_RS07540	5351.44	2.19	0.23	5.24E-22	*dnaA*	chromosomal replication initiator protein DnaA
HMPREF1322_RS01760	8591.86	2.00	0.21	2.09E-21	-	electron transfer flavoprotein subunit alpha/FixB family protein
HMPREF1322_RS02075	76668.23	2.38	0.25	7.17E-21	*rpsO*	30S ribosomal protein S15
HMPREF1322_RS07695	18257.75	2.38	0.26	1.73E-20	-	50S ribosomal protein L28
HMPREF1322_RS07305	39671.02	3.52	0.38	3.70E-20	-	SDR family oxidoreductase
HMPREF1322_RS06590	3693.30	2.34	0.26	7.00E-20	-	lipoprotein signal peptidase
HMPREF1322_RS04880	1646.03	2.96	0.33	7.77E-20	-	electron transport complex subunit E
HMPREF1322_RS07315	10873.97	2.21	0.24	2.04E-19	*pdxA*	4-hydroxythreonine-4-phosphate dehydrogenase PdxA
HMPREF1322_RS02115	802.74	3.67	0.41	3.12E-19	-	thiazole synthase
HMPREF1322_RS04430	6944.22	2.67	0.30	4.81E-19	*vorB*	3-methyl-2-oxobutanoate dehydrogenase subunit VorB
HMPREF1322_RS06505	6503.86	2.28	0.26	4.99E-19	-	succinate dehydrogenase/fumarate reductase cytochrome b subunit
HMPREF1322_RS01420	4037.78	2.32	0.27	2.55E-18	-	peptide chain release factor 2
HMPREF1322_RS06515	17162.15	1.98	0.23	4.65E-18	-	succinate dehydrogenase/fumarate reductase iron-sulfur subunit
HMPREF1322_RS06545	9763.98	2.91	0.35	5.41E-17	-	sodium ion-translocating decarboxylase subunit beta
HMPREF1322_RS07560	1584.83	1.91	0.23	6.14E-17	-	hypothetical protein
HMPREF1322_RS04870	2568.12	2.33	0.28	7.12E-17	-	RnfABCDGE type electron transport complex subunit D
HMPREF1322_RS09385	113129.22	4.77	0.57	7.41E-17	-	tRNA-Ile
HMPREF1322_RS01415	5871.99	1.89	0.23	8.89E-17	-	long-chain fatty acid--CoA ligase
HMPREF1322_RS04445	1892.04	2.05	0.25	1.71E-16	-	2-oxoglutarate ferredoxin oxidoreductase subunit gamma
HMPREF1322_RS03105	19942.29	2.37	0.29	2.99E-16	*mazG*	nucleoside triphosphate pyrophosphohydrolase
HMPREF1322_RS02105	2652.52	2.90	0.36	6.36E-16	*thiC*	phosphomethylpyrimidine synthase ThiC
HMPREF1322_RS07295	918.07	2.53	0.32	1.25E-15	-	hypothetical protein

LFC: log_2 fold change
lfcSE: Standard error of log_2 fold change

Table 2. Genes most under-expressed in excess hemin conditions (or most over-expressed in limited hemin conditions) ordered by their significance P-value. The complete list of 268 genes is included in S2 Table.

Locus Tag	baseMean	LFC	lfcSE	P-value	Gene Symbol	Gene Product
HMPREF1322_RS06000	19212.04	-7.71	0.27	1.21E-184	-	TetR/AcrR family transcriptional regulator
HMPREF1322_RS06010	7387.12	-8.06	0.28	5.34E-183	-	outer membrane lipoprotein-sorting protein
HMPREF1322_RS06015	24454.31	-7.46	0.28	2.46E-160	-	hypothetical protein
HMPREF1322_RS06005	47425.12	-7.36	0.30	1.87E-133	-	MMPL family transporter
HMPREF1322_RS05430	7754.25	-5.44	0.23	7.95E-121	-	flavodoxin
HMPREF1322_RS06790	15141.08	-6.11	0.30	3.67E-92	-	heme-binding protein HmuY
HMPREF1322_RS04145	4231.05	-5.42	0.29	7.09E-76	-	DUF4876 domain-containing protein
HMPREF1322_RS00165	33997.53	-3.86	0.24	3.60E-60	-	hypothetical protein
HMPREF1322_RS08955	18702.05	-3.75	0.23	6.92E-59	-	PglZ domain-containing protein
HMPREF1322_RS03170	5510.46	-5.17	0.32	2.13E-57	-	T9SS type A sorting domain-containing protein
HMPREF1322_RS00745	3619.54	-4.27	0.27	2.40E-57	-	ABC transporter ATP-binding protein
HMPREF1322_RS00465	1031.56	-4.52	0.29	2.04E-55	-	DUF3575 domain-containing protein
HMPREF1322_RS03855	47852.31	-3.81	0.25	8.15E-51	-	T9SS type A sorting domain-containing protein
HMPREF1322_RS05045	1138.34	-4.32	0.29	5.25E-50	-	hypothetical protein
HMPREF1322_RS07370	25172.29	-3.07	0.21	1.50E-47	-	transposase
HMPREF1322_RS05050	901.14	-3.69	0.26	5.74E-47	-	hypothetical protein
HMPREF1322_RS04140	4263.72	-5.40	0.39	9.54E-44	-	TonB-dependent receptor
HMPREF1322_RS07285	4362.71	-3.54	0.26	1.81E-42	-	IS5/IS1182 family transposase
HMPREF1322_RS00730	1091.42	-3.38	0.25	5.01E-41	-	hypothetical protein
HMPREF1322_RS10850	767.65	-3.04	0.23	6.51E-41	-	IS5/IS1182 family transposase
HMPREF1322_RS05700	1363.75	-2.92	0.22	6.42E-39	-	IS5/IS1182 family transposase
HMPREF1322_RS02830	245.42	-3.57	0.27	1.53E-38	-	helix-turn-helix domain-containing protein
HMPREF1322_RS08255	1559.13	-2.94	0.23	2.65E-38	-	IS5/IS1182 family transposase
HMPREF1322_RS00725	911.64	-2.93	0.23	5.26E-38	-	lactate utilization protein
HMPREF1322_RS05425	530.83	-3.76	0.29	1.83E-37	-	DUF2023 family protein
HMPREF1322_RS00485	425.30	-3.46	0.27	2.24E-37	-	DUF4906 domain-containing protein
HMPREF1322_RS07380	45140.22	-3.08	0.24	3.93E-37	-	family outer membrane protein
HMPREF1322_RS08605	2232.06	-4.56	0.36	4.87E-37	-	co-chaperone GroES
HMPREF1322_RS07630	1708.56	-3.97	0.31	5.27E-37	-	class I SAM-dependent methyltransferase
HMPREF1322_RS04045	1062.32	-2.77	0.22	1.27E-36	-	IS982 family transposase

LFC: log_2 fold change
lfcSE: Standard error of log_2 fold change

Table 3. DMAs (6mA) identified in *P. gingivalis* W50, selecting for a minimum mean 5% methylation difference between experimental conditions (FDR = 5% and minimum 10× coverage).

Contig	Position	Strand	mean % methylation: LiH	mean % methylation: ExH	% methylation difference	P-value	Gene ID (Locus Tag)	Gene Symbol	Gene Product	Gene on the same strand	Genes ± 1 kb away, both strands
NZ_AJZS01000047.1	40035	-	71.83%	77.08%	5.25%	7.49E-08	HMPREF1322_RS04255	*thrS*	threonine—tRNA ligase	No	HMPREF1322_RS04255
NZ_AJZS01000038.1	3559	-	4.43%	89.64%	85.21%	7.67E-08	HMPREF1322_RS03650	-	4-alpha-glucanotransferase	Yes	HMPREF1322_RS03645,HMPREF1322_RS03650
NZ_AJZS01000050.1	55602	+	53.36%	63.37%	10.01%	1.98E-07	HMPREF1322_RS04535	-	aminopeptidase	No	HMPREF1322_RS04535,HMPREF1322_RS10055
NZ_AJZS01000066.1	22242	-	15.95%	96.80%	80.86%	3.66E-07	HMPREF1322_RS06180	-	Ppx/GppA family phosphatase	Yes	HMPREF1322_RS06175,HMPREF1322_RS06180
NZ_AJZS01000011.1	13584	+	2.40%	14.66%	12.25%	5.18E-07	HMPREF1322_RS00725	-	lactate utilization protein	Yes	HMPREF1322_RS00720,HMPREF1322_RS00725, HMPREF1322_RS00730
NZ_AJZS01000009.1	24820	-	0.00%	6.32%	6.32%	1.07E-06	HMPREF1322_RS00645	*pckA*	phosphoenolpyruvate carboxykinase (ATP)	No	HMPREF1322_RS00645,HMPREF1322_RS00650, HMPREF1322_RS00655
NZ_AJZS01000097.1	917	+	6.32%	0.00%	6.32%	1.07E-06	HMPREF1322_RS09020	-	lipid A deacylase	No	HMPREF1322_RS09015,HMPREF1322_RS09020, HMPREF1322_RS09025
NZ_AJZS01000099.1	2869	-	55.68%	47.10%	8.58%	1.41E-06	-	-	-	-	HMPREF1322_RS09365,HMPREF1322_RS09370, HMPREF1322_RS09375
NZ_AJZS01000011.1	14744	+	2.00%	28.52%	26.52%	1.52E-06	HMPREF1322_RS00730	-	hypothetical protein	Yes	HMPREF1322_RS00725,HMPREF1322_RS00730, HMPREF1322_RS00735
NZ_AJZS01000020.1	1186	+	6.83%	0.00%	6.83%	1.66E-06	HMPREF1322_RS01925	-	histidinol-phosphate aminotransferase	Yes	HMPREF1322_RS01920,HMPREF1322_RS09820, HMPREF1322_RS01925
NZ_AJZS01000048.1	5988	-	0.00%	8.01%	8.01%	1.70E-06	HMPREF1322_RS10675	-	hypothetical protein	No	HMPREF1322_RS04285,HMPREF1322_RS10675, HMPREF1322_RS04295
NZ_AJZS01000011.1	14487	+	0.97%	19.32%	18.35%	2.62E-06	HMPREF1322_RS00730	-	hypothetical protein	Yes	HMPREF1322_RS00725,HMPREF1322_RS00730, HMPREF1322_RS00735
NZ_AJZS01000091.1	1018	-	16.24%	0.00%	16.24%	2.94E-06	HMPREF1322_RS08515	-	8-amino-7-oxono-noate synthase	No	HMPREF1322_RS08515
NZ_AJZS01000011.1	14511	+	4.96%	46.35%	41.39%	3.60E-06	HMPREF1322_RS00730	-	hypothetical protein	Yes	HMPREF1322_RS00725,HMPREF1322_RS00730, HMPREF1322_RS00735
NZ_AJZS01000011.1	14324	+	1.76%	17.10%	15.34%	3.75E-06	HMPREF1322_RS00725	-	lactate utilization protein	Yes	HMPREF1322_RS00725,HMPREF1322_RS00730, HMPREF1322_RS00735
NZ_AJZS01000067.1	34053	-	34.85%	21.64%	13.21%	4.13E-06	HMPREF1322_RS06415	*porQ*	type IX secretion system protein PorQ	Yes	HMPREF1322_RS06405,HMPREF1322_RS06410, HMPREF1322_RS06415
NZ_AJZS01000011.1	13965	+	3.83%	37.85%	34.02%	4.16E-06	HMPREF1322_RS00725	-	lactate utilization protein	Yes	HMPREF1322_RS00720,HMPREF1322_RS00725, HMPREF1322_RS00730
NZ_AJZS01000011.1	14644	+	5.20%	29.07%	23.87%	4.28E-06	HMPREF1322_RS00730	-	hypothetical protein	Yes	HMPREF1322_RS00725,HMPREF1322_RS00730, HMPREF1322_RS00735
NZ_AJZS01000066.1	22938	-	85.99%	37.41%	48.59%	4.56E-06	HMPREF1322_RS06180	-	Ppx/GppA family phosphatase	Yes	HMPREF1322_RS06175,HMPREF1322_RS06180, HMPREF1322_RS06185
NZ_AJZS01000038.1	3560	-	1.45%	86.22%	84.77%	5.31E-06	HMPREF1322_RS03650	-	4-alpha-glucanotransferase	Yes	HMPREF1322_RS03645,HMPREF1322_RS03650
NZ_AJZS01000011.1	13236	+	6.84%	52.42%	45.58%	5.83E-06	HMPREF1322_RS00725	-	lactate utilization protein	Yes	HMPREF1322_RS00720,HMPREF1322_RS00725
NZ_AJZS01000071.1	5863	-	62.88%	80.42%	17.54%	6.37E-06	HMPREF1322_RS07305	-	SDR family oxidoreductase	Yes	HMPREF1322_RS07300,HMPREF1322_RS07305, HMPREF1322_RS07310,HMPREF1322_RS07315

NZ_AJZS01000029.1	4423	-	5.57%	0.00%	5.57%	6.37E-06	HMPREF1322_RS03075	-	AAA domain-containing protein	Yes	HMPREF1322_RS03070,HMPREF1322_RS03075
NZ_AJZS01000046.1	4018	-	3.69%	15.60%	11.90%	6.52E-06	HMPREF1322_RS04100	-	hypothetical protein	Yes	HMPREF1322_RS04100,HMPREF1322_RS10660
NZ_AJZS01000069.1	36533	-	13.51%	18.84%	5.33%	6.81E-06	HMPREF1322_RS06610	-	ComEC/Rec2 family competence protein	No	HMPREF1322_RS06605,HMPREF1322_RS06610
NZ_AJZS01000093.1	1666	-	34.44%	16.94%	17.50%	8.21E-06	HMPREF1322_RS08685	*pruA*	L-glutamate gamma-semialdehyde dehydrogenase	Yes	HMPREF1322_RS08685,HMPREF1322_RS08690
NZ_AJZS01000011.1	14200	+	5.92%	18.54%	12.62%	8.66E-06	HMPREF1322_RS00725	-	lactate utilization protein	Yes	HMPREF1322_RS00725,HMPREF1322_RS00730, HMPREF1322_RS00735
NZ_AJZS01000063.1	3841	-	5.37%	0.00%	5.37%	8.67E-06	-	-	-	-	HMPREF1322_RS05995
NZ_AJZS01000101.1	9445	-	50.00%	75.93%	25.93%	9.71E-06	-	-	-	-	HMPREF1322_RS09650,HMPREF1322_RS09490, HMPREF1322_RS09495
NZ_AJZS01000091.1	663	-	5.19%	0.00%	5.19%	9.98E-06	HMPREF1322_RS08515	-	8-amino-7-oxono-noate synthase	No	HMPREF1322_RS08515
NZ_AJZS01000068.1	5296	-	24.60%	41.90%	17.30%	1.10E-05	HMPREF1322_RS06440	-	glycine--tRNA- ligase	Yes	HMPREF1322_RS06440,HMPREF1322_RS06445
NZ_AJZS01000011.1	15471	+	7.97%	28.75%	20.78%	1.11E-05	HMPREF1322_RS00735	-	PaaI family thioesterase	No	HMPREF1322_RS00725,HMPREF1322_RS00730, HMPREF1322_RS00735,HMPREF1322_RS00740
NZ_AJZS01000085.1	7204	-	33.33%	59.05%	25.72%	1.12E-05	HMPREF1322_RS08155	-	M56 family metallopeptidase	No	HMPREF1322_RS08150,HMPREF1322_RS08155, HMPREF1322_RS10845
NZ_AJZS01000069.1	173248	-	37.82%	19.39%	18.43%	1.14E-05	HMPREF1322_RS07250	-	site-specific integrase	No	HMPREF1322_RS07245,HMPREF1322_RS07250, HMPREF1322_RS07255
NZ_AJZS01000011.1	19392	+	7.54%	25.19%	17.66%	1.14E-05	HMPREF1322_RS00745	-	ABC transporter ATP-binding protein	No	HMPREF1322_RS00745
NZ_AJZS01000048.1	4837	-	0.00%	9.02%	9.02%	1.15E-05	-	-	-	-	HMPREF1322_RS04280,HMPREF1322_RS04285
NZ_AJZS01000011.1	17614	+	2.76%	16.42%	13.66%	1.15E-05	HMPREF1322_RS00740	-	ABC transporter ATP-binding protein	No	HMPREF1322_RS00740,HMPREF1322_RS00745
NZ_AJZS01000046.1	4605	-	6.69%	0.00%	6.69%	1.30E-05	HMPREF1322_RS10660	-	ISAs1 family transposase	Yes	HMPREF1322_RS04100,HMPREF1322_RS10660
NZ_AJZS01000001.1	12773	+	58.09%	33.33%	24.76%	1.31E-05	HMPREF1322_RS00055	-	tryptophanase	Yes	HMPREF1322_RS00055
NZ_AJZS01000025.1	6136	+	20.06%	0.00%	20.06%	1.32E-05	HMPREF1322_RS02315	-	tetratricopeptide repeat protein	No	HMPREF1322_RS02310,HMPREF1322_RS02315
NZ_AJZS01000050.1	2012	-	39.24%	1.99%	37.26%	1.46E-05	-	-	-	-	HMPREF1322_RS04325,HMPREF1322_RS04330
NZ_AJZS01000050.1	1015	+	0.00%	16.57%	16.57%	1.47E-05	HMPREF1322_RS04325	-	DUF2436 domain-containing protein	No	HMPREF1322_RS04325
NZ_AJZS01000011.1	14019	+	1.48%	34.21%	32.73%	1.48E-05	HMPREF1322_RS00725	-	lactate utilization protein	Yes	HMPREF1322_RS00720,HMPREF1322_RS00725, HMPREF1322_RS00730
NZ_AJZS01000079.1	3864	-	76.11%	60.84%	15.27%	1.52E-05	HMPREF1322_RS07770	-	DUF3298 domain-containing protein	No	HMPREF1322_RS07770,HMPREF1322_RS07775, HMPREF1322_RS07780
NZ_AJZS01000011.1	14512	+	5.03%	41.65%	36.62%	1.56E-05	HMPREF1322_RS00730	-	hypothetical protein	Yes	HMPREF1322_RS00725,HMPREF1322_RS00730, HMPREF1322_RS00735
NZ_AJZS01000007.1	2872	-	16.32%	6.02%	10.30%	1.62E-05	-	-	-	-	HMPREF1322_RS00445,HMPREF1322_RS00450
NZ_AJZS01000011.1	14323	+	2.43%	19.81%	17.38%	1.65E-05	HMPREF1322_RS00725	-	lactate utilization protein	Yes	HMPREF1322_RS00725,HMPREF1322_RS00730, HMPREF1322_RS00735
NZ_AJZS01000017.1	23369	-	13.67%	18.77%	5.10%	1.66E-05	-	-	-	-	HMPREF1322_RS01475,HMPREF1322_RS01480, HMPREF1322_RS01485,HMPREF1322_RS01490

NZ_AJZS01000021.1	7225	+	11.70%	17.64%	5.94%	1.67E-05	HMPREF1322_RS01975	-	O-acetyl-ADP-ribose deacetylase	No	HMPREF1322_RS01970,HMPREF1322_RS01975, HMPREF1322_RS01980

LiH: growth in limited hemin
ExH: growth in excess hemin

Table 4. DMCs (5mC) identified in *P. gingivalis* W50, selecting for a minimum mean 5% methylation difference between experimental conditions (FDR = 5% and minimum 10× coverage).

Contig	Position	Strand	mean % methylation: LiH	mean % methylation: ExH	% methylation difference	P-value	Gene ID (Locus Tag)	Gene Symbol	Gene Product	Gene on the same strand	Genes ± 1 kb away, both strands
NZ_AJZS01000009.1	3668	+	12.68%	21.61%	8.93%	2.40E-05	HMPREF1322_RS00555	-	DEAD/DEAH box helicase family protein	No	HMPREF1322_RS00555,HMPREF1322_RS00560
NZ_AJZS01000011.1	12945	+	5.18%	61.79%	56.61%	2.71E-06	HMPREF1322_RS00720	-	(Fe-S)-binding protein	Yes	HMPREF1322_RS00715,HMPREF1322_RS00720, HMPREF1322_RS00725
NZ_AJZS01000011.1	12946	+	4.71%	58.08%	53.37%	2.09E-06	HMPREF1322_RS00720	-	(Fe-S)-binding protein	Yes	HMPREF1322_RS00715,HMPREF1322_RS00720, HMPREF1322_RS00725
NZ_AJZS01000011.1	13002	+	3.76%	55.38%	51.62%	3.63E-06	HMPREF1322_RS00720	-	(Fe-S)-binding protein	Yes	HMPREF1322_RS00715,HMPREF1322_RS00720, HMPREF1322_RS00725
NZ_AJZS01000011.1	13071	+	4.20%	21.99%	17.79%	4.48E-06	HMPREF1322_RS00720	-	(Fe-S)-binding protein	Yes	HMPREF1322_RS00720,HMPREF1322_RS00725
NZ_AJZS01000011.1	13178	+	7.08%	60.16%	53.08%	2.24E-06	HMPREF1322_RS00725	-	lactate utilization protein	Yes	HMPREF1322_RS00720,HMPREF1322_RS00725
NZ_AJZS01000011.1	13240	+	8.76%	43.87%	35.12%	1.61E-06	HMPREF1322_RS00725	-	lactate utilization protein	Yes	HMPREF1322_RS00720,HMPREF1322_RS00725
NZ_AJZS01000011.1	13430	+	9.65%	38.76%	29.11%	2.55E-05	HMPREF1322_RS00725	-	lactate utilization protein	Yes	HMPREF1322_RS00720,HMPREF1322_RS00725
NZ_AJZS01000011.1	13730	+	13.59%	58.15%	44.56%	1.13E-05	HMPREF1322_RS00725	-	lactate utilization protein	Yes	HMPREF1322_RS00720,HMPREF1322_RS00725, HMPREF1322_RS00730
NZ_AJZS01000011.1	14106	+	16.77%	47.36%	30.59%	7.45E-07	HMPREF1322_RS00725	-	lactate utilization protein	Yes	HMPREF1322_RS00720,HMPREF1322_RS00725, HMPREF1322_RS00730
NZ_AJZS01000011.1	14542	+	15.67%	34.20%	18.53%	8.76E-06	HMPREF1322_RS00730	-	hypothetical protein	Yes	HMPREF1322_RS00725,HMPREF1322_RS00730, HMPREF1322_RS00735
NZ_AJZS01000011.1	14669	+	7.23%	19.84%	12.61%	1.28E-05	HMPREF1322_RS00730	-	hypothetical protein	Yes	HMPREF1322_RS00725,HMPREF1322_RS00730, HMPREF1322_RS00735
NZ_AJZS01000011.1	14693	+	14.07%	38.73%	24.67%	1.77E-05	HMPREF1322_RS00730	-	hypothetical protein	Yes	HMPREF1322_RS00725,HMPREF1322_RS00730, HMPREF1322_RS00735
NZ_AJZS01000011.1	14698	+	26.82%	44.78%	17.96%	7.90E-06	HMPREF1322_RS00730	-	hypothetical protein	Yes	HMPREF1322_RS00725,HMPREF1322_RS00730, HMPREF1322_RS00735
NZ_AJZS01000011.1	14706	+	2.91%	21.70%	18.79%	1.52E-05	HMPREF1322_RS00730	-	hypothetical protein	Yes	HMPREF1322_RS00725,HMPREF1322_RS00730, HMPREF1322_RS00735
NZ_AJZS01000011.1	18653	+	4.65%	18.69%	14.04%	2.34E-05	HMPREF1322_RS00745	-	ABC transporter ATP-binding protein	No	HMPREF1322_RS00740,HMPREF1322_RS00745
NZ_AJZS01000013.1	2448	-	11.90%	17.41%	5.51%	2.20E-05	HMPREF1322_RS00790	*gyrA*	DNA gyrase subunit A	Yes	HMPREF1322_RS00785,HMPREF1322_RS00790
NZ_AJZS01000014.1	5938	+	34.76%	52.63%	17.87%	2.45E-06	HMPREF1322_RS00860	*htpG*	molecular chaperone HtpG	No	HMPREF1322_RS00860
NZ_AJZS01000015.1	78713	-	64.82%	58.15%	6.67%	1.08E-05	HMPREF1322_RS01240	-	iron ABC transporter permease	Yes	HMPREF1322_RS01240,HMPREF1322_RS01245
NZ_AJZS01000015.1	952	+	13.70%	22.02%	8.33%	6.03E-06	HMPREF1322_RS00885	-	U32 family peptidase	No	HMPREF1322_RS00880,HMPREF1322_RS00885
NZ_AJZS01000036.1	5418	+	22.76%	14.46%	8.30%	1.59E-05	HMPREF1322_RS03420	-	YjgP/YjgQ family permease	No	HMPREF1322_RS03410,HMPREF1322_RS03415, HMPREF1322_RS03420,HMPREF1322_RS03425
NZ_AJZS01000037.1	41404	-	62.40%	68.48%	6.08%	6.02E-06	HMPREF1322_RS03585	-	CusA/CzcA family heavy metal efflux RND transporter	No	HMPREF1322_RS03585,HMPREF1322_RS03590
NZ_AJZS01000038.1	3558	-	5.53%	95.22%	89.69%	4.16E-07	HMPREF1322_RS03650	-	4-alpha-glucanotransferase	Yes	HMPREF1322_RS03645,HMPREF1322_RS03650

NZ_AJZS01000039.1	305	+	6.19%	17.19%	10.99%	4.82E-06	-	-	-	-	HMPREF1322_RS03655
NZ_AJZS01000041.1	4471	-	17.52%	22.93%	5.41%	9.62E-06	-	-	-	-	HMPREF1322_RS03860,HMPREF1322_RS03870, HMPREF1322_RS03875
NZ_AJZS01000046.1	1044	-	10.78%	5.27%	5.52%	8.29E-06	HMPREF1322_RS04090	-	MBOAT family protein	Yes	HMPREF1322_RS04090,HMPREF1322_RS04095
NZ_AJZS01000047.1	30511	+	65.91%	58.49%	7.42%	1.42E-06	HMPREF1322_RS04210	-	S9 family peptidase	Yes	HMPREF1322_RS04205,HMPREF1322_RS04210
NZ_AJZS01000050.1	1569	-	53.78%	2.75%	51.03%	2.69E-06	HMPREF1322_RS04325	-	DUF2436 domain-containing protein	Yes	HMPREF1322_RS04325,HMPREF1322_RS04330
NZ_AJZS01000050.1	1612	-	34.96%	8.22%	26.74%	1.53E-06	HMPREF1322_RS04325	-	DUF2436 domain-containing protein	Yes	HMPREF1322_RS04325,HMPREF1322_RS04330
NZ_AJZS01000050.1	1624	-	31.26%	11.13%	20.13%	5.57E-06	HMPREF1322_RS04325	-	DUF2436 domain-containing protein	Yes	HMPREF1322_RS04325,HMPREF1322_RS04330
NZ_AJZS01000050.1	1625	-	26.00%	9.52%	16.48%	9.79E-06	HMPREF1322_RS04325	-	DUF2436 domain-containing protein	Yes	HMPREF1322_RS04325,HMPREF1322_RS04330
NZ_AJZS01000050.1	1769	-	49.12%	2.56%	46.56%	2.20E-05	-	-	-	-	HMPREF1322_RS04325,HMPREF1322_RS04330
NZ_AJZS01000050.1	1920	-	64.72%	8.39%	56.32%	7.23E-06	-	-	-	-	HMPREF1322_RS04325,HMPREF1322_RS04330
NZ_AJZS01000050.1	2002	-	58.99%	4.81%	54.18%	1.57E-05	-	-	-	-	HMPREF1322_RS04325,HMPREF1322_RS04330
NZ_AJZS01000050.1	2099	-	58.19%	8.09%	50.10%	6.00E-06	HMPREF1322_RS04330	-	nucleoside permease	Yes	HMPREF1322_RS04325,HMPREF1322_RS04330
NZ_AJZS01000050.1	2101	-	53.34%	4.65%	48.69%	1.74E-05	HMPREF1322_RS04330	-	nucleoside permease	Yes	HMPREF1322_RS04325,HMPREF1322_RS04330
NZ_AJZS01000050.1	2103	-	61.60%	6.56%	55.04%	2.66E-05	HMPREF1322_RS04330	-	nucleoside permease	Yes	HMPREF1322_RS04325,HMPREF1322_RS04330
NZ_AJZS01000050.1	2262	-	53.40%	9.81%	43.59%	1.20E-05	HMPREF1322_RS04330	-	nucleoside permease	Yes	HMPREF1322_RS04325,HMPREF1322_RS04330
NZ_AJZS01000050.1	797	-	38.96%	13.79%	25.16%	2.31E-05	HMPREF1322_RS04325	-	DUF2436 domain-containing protein	Yes	HMPREF1322_RS04325
NZ_AJZS01000066.1	22243	-	10.21%	64.13%	53.91%	6.11E-07	HMPREF1322_RS06180	-	Ppx/GppA family phosphatase	Yes	HMPREF1322_RS06175,HMPREF1322_RS06180
NZ_AJZS01000066.1	22943	+	70.43%	31.90%	38.53%	2.21E-05	HMPREF1322_RS06180	-	Ppx/GppA family phosphatase	No	HMPREF1322_RS06175,HMPREF1322_RS06180, HMPREF1322_RS06185
NZ_AJZS01000069.1	3434	-	51.80%	41.48%	10.32%	1.97E-05	HMPREF1322_RS06465	-	hypothetical protein	Yes	HMPREF1322_RS06460,HMPREF1322_RS06465, HMPREF1322_RS06470
NZ_AJZS01000080.1	123	+	12.46%	0.00%	12.46%	1.76E-05	HMPREF1322_RS07835	-	hypothetical protein	Yes	HMPREF1322_RS07835,HMPREF1322_RS07840, HMPREF1322_RS07845
NZ_AJZS01000080.1	124	+	12.46%	0.00%	12.46%	1.76E-05	HMPREF1322_RS07835	-	hypothetical protein	Yes	HMPREF1322_RS07835,HMPREF1322_RS07840, HMPREF1322_RS07845
NZ_AJZS01000089.1	26	+	0.00%	9.03%	9.03%	1.34E-05	HMPREF1322_RS08455	-	IS5/IS1182 family transposase	Yes	HMPREF1322_RS08455,HMPREF1322_RS08460
NZ_AJZS01000102.1	6840	-	6.63%	12.27%	5.64%	3.39E-07	HMPREF1322_RS09535	-	pyridoxal phosphate-dependent aminotransferase	Yes	HMPREF1322_RS09535,HMPREF1322_RS09540
NZ_AJZS01000104.1	8834	-	0.00%	7.90%	7.90%	3.17E-06	HMPREF1322_RS09610	-	tetratricopeptide repeat protein	Yes	HMPREF1322_RS09605,HMPREF1322_RS09610

LiH: growth in limited hemin
ExH: growth in excess hemin

Table 5. Genes overexpressed in excess hemin conditions with DMAs (> 1.5 LFC, > 5% methylation difference, FDR = 5%).

Locus Tag	Gene Symbol	Gene Product	Contig	Gene start	Gene end	Strand Expr.	Methylated Position	Strand Meth.	Distance Meth.	DE analysis			DM analysis			
										baseMean	LFC	P-value	mean % methylation: LiH	mean % methylation: ExH	% methylation difference	P-value
HMPREF1322_RS07305	-	SDR family oxidoreductase	NZ_AJZS01000071.1	5169	5900	-	5863	-	694	39671.02	3.52	3.70E-20	62.88%	80.42%	17.54%	6.37E-06
HMPREF1322_RS07315	*pdxA*	4-hydroxythreonine-4-phosphate dehydrogenase PdxA	NZ_AJZS01000071.1	6386	7483	-	5863	-	-523	10873.97	2.21	2.04E-19	62.88%	80.42%	17.54%	6.37E-06
HMPREF1322_RS06180	-	Ppx/GppA family phosphatase	NZ_AJZS01000066.1	22201	23108	-	22242	-	41	914.83	1.59	2.19E-12	15.95%	96.80%	80.86%	3.66E-07
HMPREF1322_RS06180	-	Ppx/GppA family phosphatase	NZ_AJZS01000066.1	22201	23108	-	22938	-	737	914.83	1.59	2.19E-12	85.99%	37.41%	48.59%	4.56E-06
HMPREF1322_RS01480	-	tRNA-Thr	NZ_AJZS01000017.1	23424	23496	-	23369	-	-55	362.80	2.29	2.35E-12	13.67%	18.77%	5.10%	1.66E-05
HMPREF1322_RS01485	-	hypothetical protein	NZ_AJZS01000017.1	23557	24009	-	23369	-	-188	2236.75	2.55	9.57E-12	13.67%	18.77%	5.10%	1.66E-05
HMPREF1322_RS04280	*dnaE*	DNA polymerase III subunit alpha	NZ_AJZS01000048.1	883	4569	-	4837	-	3954	4976.97	1.52	1.59E-09	0.00%	9.02%	9.02%	1.15E-05
HMPREF1322_RS04100	-	hypothetical protein	NZ_AJZS01000046.1	2632	4023	-	4018	-	1386	3442.27	1.59	9.47E-09	3.69%	15.60%	11.90%	6.52E-06
HMPREF1322_RS04100	-	hypothetical protein	NZ_AJZS01000046.1	2632	4023	-	4605	-	1973	3442.27	1.59	9.47E-09	6.69%	0.00%	6.69%	1.30E-05
HMPREF1322_RS09370	*rrf*	5S ribosomal RNA	NZ_AJZS01000099.1	3390	3500	-	2869	-	-521	5793.67	1.71	6.69E-04	55.68%	47.10%	8.58%	1.41E-06

Strand Expr: Strand of the gene
Strand Meth: Strand of the methylated position
Distance Meth: Distance of the methylated position to the gene start site in base pairs, negative values indicate upstream location
DE analysis: results from the differential expression analysis
DM analysis: results from the differential methylation analysis
LFC: log_2 fold change
LiH: growth in limited hemin
ExH: growth in excess hemin

Table 6. Genes under-expressed in excess hemin conditions with DMAs (< -1.5 LFC, > 5% methylation difference, FDR = 5%).

Locus Tag	Gene Symbol	Gene Product	Contig	Gene start	Gene end	Strand Expr.	Methylated Position	Strand Meth.	Distance Meth.	DE analysis			DM analysis			
										baseMean	LFC	P-value	mean % methylation: LiH	mean % methylation: ExH	% methylation difference	P-value
HMPREF1322_RS00745	-	ABC transporter ATP-binding protein	NZ_AJZS01000011.1	17886	19607	-	17614	+	-272	3619.54	-4.27	2.40E-57	2.76%	16.42%	13.66%	1.15E-05
HMPREF1322_RS00745	-	ABC transporter ATP-binding protein	NZ_AJZS01000011.1	17886	19607	-	19392	+	1506	3619.54	-4.27	2.40E-57	7.54%	25.19%	17.66%	1.14E-05
HMPREF1322_RS00730	-	hypothetical protein	NZ_AJZS01000011.1	14478	15062	+	13584	+	-894	1091.42	-3.38	5.01E-41	2.40%	14.66%	12.25%	5.18E-07
HMPREF1322_RS00730	-	hypothetical protein	NZ_AJZS01000011.1	14478	15062	+	13965	+	-513	1091.42	-3.38	5.01E-41	3.83%	37.85%	34.02%	4.16E-06
HMPREF1322_RS00730	-	hypothetical protein	NZ_AJZS01000011.1	14478	15062	+	14019	+	-459	1091.42	-3.38	5.01E-41	1.48%	34.21%	32.73%	1.48E-05
HMPREF1322_RS00730	-	hypothetical protein	NZ_AJZS01000011.1	14478	15062	+	14200	+	-278	1091.42	-3.38	5.01E-41	5.92%	18.54%	12.62%	8.66E-06
HMPREF1322_RS00730	-	hypothetical protein	NZ_AJZS01000011.1	14478	15062	+	14323	+	-155	1091.42	-3.38	5.01E-41	2.43%	19.81%	17.38%	1.65E-05
HMPREF1322_RS00730	-	hypothetical protein	NZ_AJZS01000011.1	14478	15062	+	14324	+	-154	1091.42	-3.38	5.01E-41	1.76%	17.10%	15.34%	3.75E-06
HMPREF1322_RS00730	-	hypothetical protein	NZ_AJZS01000011.1	14478	15062	+	14487	+	9	1091.42	-3.38	5.01E-41	0.97%	19.32%	18.35%	2.62E-06
HMPREF1322_RS00730	-	hypothetical protein	NZ_AJZS01000011.1	14478	15062	+	14511	+	33	1091.42	-3.38	5.01E-41	4.96%	46.35%	41.39%	3.60E-06
HMPREF1322_RS00730	-	hypothetical protein	NZ_AJZS01000011.1	14478	15062	+	14512	+	34	1091.42	-3.38	5.01E-41	5.03%	41.65%	36.62%	1.56E-05
HMPREF1322_RS00730	-	hypothetical protein	NZ_AJZS01000011.1	14478	15062	+	14644	+	166	1091.42	-3.38	5.01E-41	5.20%	29.07%	23.87%	4.28E-06
HMPREF1322_RS00730	-	hypothetical protein	NZ_AJZS01000011.1	14478	15062	+	14744	+	266	1091.42	-3.38	5.01E-41	2.00%	28.52%	26.52%	1.52E-06
HMPREF1322_RS00730	-	hypothetical protein	NZ_AJZS01000011.1	14478	15062	+	15471	+	993	1091.42	-3.38	5.01E-41	7.97%	28.75%	20.78%	1.11E-05
HMPREF1322_RS00725	-	lactate utilization protein	NZ_AJZS01000011.1	13105	14472	+	13236	+	131	911.64	-2.93	5.26E-38	6.84%	52.42%	45.58%	5.83E-06
HMPREF1322_RS00725	-	lactate utilization protein	NZ_AJZS01000011.1	13105	14472	+	13584	+	479	911.64	-2.93	5.26E-38	2.40%	14.66%	12.25%	5.18E-07
HMPREF1322_RS00725	-	lactate utilization protein	NZ_AJZS01000011.1	13105	14472	+	13965	+	860	911.64	-2.93	5.26E-38	3.83%	37.85%	34.02%	4.16E-06
HMPREF1322_RS00725	-	lactate utilization protein	NZ_AJZS01000011.1	13105	14472	+	14019	+	914	911.64	-2.93	5.26E-38	1.48%	34.21%	32.73%	1.48E-05
HMPREF1322_RS00725	-	lactate utilization protein	NZ_AJZS01000011.1	13105	14472	+	14200	+	1095	911.64	-2.93	5.26E-38	5.92%	18.54%	12.62%	8.66E-06
HMPREF1322_RS00725	-	lactate utilization protein	NZ_AJZS01000011.1	13105	14472	+	14323	+	1218	911.64	-2.93	5.26E-38	2.43%	19.81%	17.38%	1.65E-05
HMPREF1322_RS00725	-	lactate utilization protein	NZ_AJZS01000011.1	13105	14472	+	14324	+	1219	911.64	-2.93	5.26E-38	1.76%	17.10%	15.34%	3.75E-06

HMPREF1322_RS00725	-	lactate utilization protein	NZ_AJZS01000011.1	13105	14472	+	14487	+	1382	911.64	-2.93	5.26E-38	0.97%	19.32%	18.35%	2.62E-06
HMPREF1322_RS00725	-	lactate utilization protein	NZ_AJZS01000011.1	13105	14472	+	14511	+	1406	911.64	-2.93	5.26E-38	4.96%	46.35%	41.39%	3.60E-06
HMPREF1322_RS00725	-	lactate utilization protein	NZ_AJZS01000011.1	13105	14472	+	14512	+	1407	911.64	-2.93	5.26E-38	5.03%	41.65%	36.62%	1.56E-05
HMPREF1322_RS00725	-	lactate utilization protein	NZ_AJZS01000011.1	13105	14472	+	14644	+	1539	911.64	-2.93	5.26E-38	5.20%	29.07%	23.87%	4.28E-06
HMPREF1322_RS00725	-	lactate utilization protein	NZ_AJZS01000011.1	13105	14472	+	14744	+	1639	911.64	-2.93	5.26E-38	2.00%	28.52%	26.52%	1.52E-06
HMPREF1322_RS00725	-	lactate utilization protein	NZ_AJZS01000011.1	13105	14472	+	15471	+	2366	911.64	-2.93	5.26E-38	7.97%	28.75%	20.78%	1.11E-05
HMPREF1322_RS01975	-	O-acetyl-ADP-ribose deacetylase	NZ_AJZS01000021.1	7184	7678	-	7225	+	41	6623.03	-2.30	2.87E-18	11.70%	17.64%	5.94%	1.67E-05
HMPREF1322_RS02315	-	tetratricopeptide repeat protein	NZ_AJZS01000025.1	5372	7181	-	6136	+	764	11707.30	-3.03	4.40E-17	20.06%	0.00%	20.06%	1.32E-05
HMPREF1322_RS03650	-	4-alpha-glucanotransferase	NZ_AJZS01000038.1	2961	4847	-	3559	-	598	5951.70	-2.22	5.69E-14	4.43%	89.64%	85.21%	7.67E-08
HMPREF1322_RS03650	-	4-alpha-glucanotransferase	NZ_AJZS01000038.1	2961	4847	-	3560	-	599	5951.70	-2.22	5.69E-14	1.45%	86.22%	84.77%	5.31E-06
HMPREF1322_RS02310	-	response regulator transcription factor	NZ_AJZS01000025.1	4676	5359	-	6136	+	1460	10536.03	-1.99	1.34E-13	20.06%	0.00%	20.06%	1.32E-05
HMPREF1322_RS01980	-	UDP-2,3-diacylglucosamine diphosphatase	NZ_AJZS01000021.1	7760	8548	-	7225	+	-535	13336.64	-1.78	2.46E-13	11.70%	17.64%	5.94%	1.67E-05
HMPREF1322_RS07250	-	site-specific integrase	NZ_AJZS01000069.1	173000	174202	+	173248	-	248	320.75	-1.58	8.34E-11	37.82%	19.39%	18.43%	1.14E-05
HMPREF1322_RS00740	-	ABC transporter ATP-binding protein	NZ_AJZS01000011.1	16133	17839	-	15471	+	-662	7059.72	-2.68	5.06E-10	7.97%	28.75%	20.78%	1.11E-05
HMPREF1322_RS00740	-	ABC transporter ATP-binding protein	NZ_AJZS01000011.1	16133	17839	-	17614	+	1481	7059.72	-2.68	5.06E-10	2.76%	16.42%	13.66%	1.15E-05
HMPREF1322_RS09495	-	hypothetical protein	NZ_AJZS01000101.1	10189	10749	+	9445	-	-744	6645.00	-2.53	3.50E-09	50.00%	75.93%	25.93%	9.71E-06
HMPREF1322_RS07780	-	MBL fold metallo-hydrolase	NZ_AJZS01000079.1	4600	5244	+	3864	-	-736	2319.58	-2.32	2.51E-06	76.11%	60.84%	15.27%	1.52E-05
HMPREF1322_RS08150	-	BlaI/MecI/CopY family transcriptional regulator	NZ_AJZS01000085.1	6031	6411	+	7204	-	1173	403.18	-1.74	2.90E-06	33.33%	59.05%	25.72%	1.12E-05
HMPREF1322_RS10055	-	hypothetical protein	NZ_AJZS01000050.1	56011	56172	+	55602	+	-409	18.27	-1.91	7.10E-04	53.36%	63.37%	10.01%	1.98E-07
HMPREF1322_RS09820	-	hypothetical protein	NZ_AJZS01000020.1	830	1045	+	1186	+	356	251.64	-1.72	1.04E-03	6.83%	0.00%	6.83%	1.66E-06

Strand Expr: Strand of the gene

Strand Meth: Strand of the methylated position

Distance Meth: Distance of the methylated position to the gene start site in base pairs, negative values indicate upstream location

DE analysis: results from the differential expression analysis

DM analysis: results from the differential methylation analysis
LFC: log_2 fold change
LiH: growth in limited hemin
ExH: growth in excess hemin

Table 7. Genes over-expressed in excess hemin conditions with DMCs (> 1.5 LFC, > 5% methylation difference, FDR = 5%).

Locus Tag	Gene Symbol	Gene Product	Contig	Gene start	Gene end	Strand Expr.	Methylated Position	Strand Meth.	Distance Meth.	DE analysis			DM analysis			
										baseMean	LFC	P-value	mean % methylation: LiH	mean % methylation: ExH	% methylation difference	P-value
HMPREF1322_RS06180	-	Ppx/GppA family phosphatase	NZ_AJZS01000066.1	22201	23108	-	22243	-	42	914.83	1.59	2.19E-12	10.21%	64.13%	53.91%	6.11E-07
HMPREF1322_RS06180	-	Ppx/GppA family phosphatase	NZ_AJZS01000066.1	22201	23108	-	22943	+	742	914.83	1.59	2.19E-12	70.43%	31.90%	38.53%	2.21E-05

Strand Expr: Strand of the gene
Strand Meth: Strand of the methylated position
Distance Meth: Distance of the methylated position to the gene start site in base pairs, negative values indicate upstream location
DE analysis: results from the differential expression analysis
DM analysis: results from the differential methylation analysis
LFC: log_2 fold change
LiH: growth in limited hemin
ExH: growth in excess hemin

Table 8. Genes under-expressed in excess hemin conditions with DMCs (< -1.5 LFC, > 5% methylation difference, FDR = 5%).

Locus Tag	Gene Symbol	Gene Product	Contig	Gene start	Gene end	Strand Expr.	Methylated Position	Strand Meth.	Distance Meth.	DE analysis			DM analysis			
										baseMean	LFC	P-value	mean % methylation: LiH	mean % methylation: ExH	% methylation difference	P-value
HMPREF1322_RS00745	-	ABC transporter ATP-binding protein	NZ_AJZS01000011.1	17886	19607	-	18653	+	767	3619.54	-4.27	2.40E-57	4.65%	18.69%	14.04%	2.34E-05
HMPREF1322_RS00730	-	hypothetical protein	NZ_AJZS01000011.1	14478	15062	+	13730	+	-748	1091.42	-3.38	5.01E-41	13.59%	58.15%	44.56%	1.13E-05
HMPREF1322_RS00730	-	hypothetical protein	NZ_AJZS01000011.1	14478	15062	+	14106	+	-372	1091.42	-3.38	5.01E-41	16.77%	47.36%	30.59%	7.45E-07
HMPREF1322_RS00730	-	hypothetical protein	NZ_AJZS01000011.1	14478	15062	+	14542	+	64	1091.42	-3.38	5.01E-41	15.67%	34.20%	18.53%	8.76E-06
HMPREF1322_RS00730	-	hypothetical protein	NZ_AJZS01000011.1	14478	15062	+	14669	+	191	1091.42	-3.38	5.01E-41	7.23%	19.84%	12.61%	1.28E-05
HMPREF1322_RS00730	-	hypothetical protein	NZ_AJZS01000011.1	14478	15062	+	14693	+	215	1091.42	-3.38	5.01E-41	14.07%	38.73%	24.67%	1.77E-05
HMPREF1322_RS00730	-	hypothetical protein	NZ_AJZS01000011.1	14478	15062	+	14698	+	220	1091.42	-3.38	5.01E-41	26.82%	44.78%	17.96%	7.90E-06
HMPREF1322_RS00730	-	hypothetical protein	NZ_AJZS01000011.1	14478	15062	+	14706	+	228	1091.42	-3.38	5.01E-41	2.91%	21.70%	18.79%	1.52E-05
HMPREF1322_RS00725	-	lactate utilization protein	NZ_AJZS01000011.1	13105	14472	+	12945	+	-160	911.64	-2.93	5.26E-38	5.18%	61.79%	56.61%	2.71E-06
HMPREF1322_RS00725	-	lactate utilization protein	NZ_AJZS01000011.1	13105	14472	+	12946	+	-159	911.64	-2.93	5.26E-38	4.71%	58.08%	53.37%	2.09E-06
HMPREF1322_RS00725	-	lactate utilization protein	NZ_AJZS01000011.1	13105	14472	+	13002	+	-103	911.64	-2.93	5.26E-38	3.76%	55.38%	51.62%	3.63E-06
HMPREF1322_RS00725	-	lactate utilization protein	NZ_AJZS01000011.1	13105	14472	+	13071	+	-34	911.64	-2.93	5.26E-38	4.20%	21.99%	17.79%	4.48E-06
HMPREF1322_RS00725	-	lactate utilization protein	NZ_AJZS01000011.1	13105	14472	+	13178	+	73	911.64	-2.93	5.26E-38	7.08%	60.16%	53.08%	2.24E-06
HMPREF1322_RS00725	-	lactate utilization protein	NZ_AJZS01000011.1	13105	14472	+	13240	+	135	911.64	-2.93	5.26E-38	8.76%	43.87%	35.12%	1.61E-06
HMPREF1322_RS00725	-	lactate utilization protein	NZ_AJZS01000011.1	13105	14472	+	13430	+	325	911.64	-2.93	5.26E-38	9.65%	38.76%	29.11%	2.55E-05
HMPREF1322_RS00725	-	lactate utilization protein	NZ_AJZS01000011.1	13105	14472	+	13730	+	625	911.64	-2.93	5.26E-38	13.59%	58.15%	44.56%	1.13E-05
HMPREF1322_RS00725	-	lactate utilization protein	NZ_AJZS01000011.1	13105	14472	+	14106	+	1001	911.64	-2.93	5.26E-38	16.77%	47.36%	30.59%	7.45E-07
HMPREF1322_RS00725	-	lactate utilization protein	NZ_AJZS01000011.1	13105	14472	+	14542	+	1437	911.64	-2.93	5.26E-38	15.67%	34.20%	18.53%	8.76E-06
HMPREF1322_RS00725	-	lactate utilization protein	NZ_AJZS01000011.1	13105	14472	+	14669	+	1564	911.64	-2.93	5.26E-38	7.23%	19.84%	12.61%	1.28E-05
HMPREF1322_RS00725	-	lactate utilization protein	NZ_AJZS01000011.1	13105	14472	+	14693	+	1588	911.64	-2.93	5.26E-38	14.07%	38.73%	24.67%	1.77E-05
HMPREF1322_RS00725	-	lactate utilization protein	NZ_AJZS01000011.1	13105	14472	+	14698	+	1593	911.64	-2.93	5.26E-38	26.82%	44.78%	17.96%	7.90E-06

HMPREF1322_RS00725	-	lactate utilization protein	NZ_AJZS01000011.1	13105	14472	+	14706	+	1601	911.64	-2.93	5.26E-38	2.91%	21.70%	18.79%	1.52E-05
HMPREF1322_RS00885	-	U32 family peptidase	NZ_AJZS01000015.1	486	2393	-	952	+	466	3114.91	-3.09	3.14E-27	13.70%	22.02%	8.33%	6.03E-06
HMPREF1322_RS00860	*htpG*	molecular chaperone HtpG	NZ_AJZS01000014.1	5016	7070	-	5938	+	922	15163.58	-2.87	2.96E-23	34.76%	52.63%	17.87%	2.45E-06
HMPREF1322_RS06465	-	hypothetical protein	NZ_AJZS01000069.1	2552	3754	-	3434	-	882	153316.28	-2.35	1.18E-19	51.80%	41.48%	10.32%	1.97E-05
HMPREF1322_RS03650	-	4-alpha-glucanotransferase	NZ_AJZS01000038.1	2961	4847	-	3558	-	597	5951.70	-2.22	5.69E-14	5.53%	95.22%	89.69%	4.16E-07
HMPREF1322_RS06460	-	transporter	NZ_AJZS01000069.1	784	2448	-	3434	-	2650	37619.48	-2.01	1.02E-13	51.80%	41.48%	10.32%	1.97E-05
HMPREF1322_RS00740	-	ABC transporter ATP-binding protein	NZ_AJZS01000011.1	16133	17839	-	18653	+	2520	7059.72	-2.68	5.06E-10	4.65%	18.69%	14.04%	2.34E-05
HMPREF1322_RS03860	-	histidinol phosphate phosphatase	NZ_AJZS01000041.1	3824	4342	-	4471	-	647	15144.78	-1.52	1.09E-09	17.52%	22.93%	5.41%	9.62E-06
HMPREF1322_RS00880	-	DUF1661 domain-containing protein	NZ_AJZS01000015.1	1	203	-	952	+	951	129.52	-1.93	8.19E-07	13.70%	22.02%	8.33%	6.03E-06

Strand Expr: Strand of the gene
Strand Meth: Strand of the methylated position
Distance Meth: Distance of the methylated position to the gene start site in base pairs, negative values indicate upstream location
DE analysis: results from the differential expression analysis
DM analysis: results from the differential methylation analysis
LFC: log_2 fold change
LiH: growth in limited hemin
ExH: growth in excess hemin

Table 9. Differentially expressed genes with DMAs and DMCs in excess hemin conditions (< -1.5 LFC, > 5% methylation difference, FDR = 5%).

Locus Tag	Gene Symbol	Gene Product	Contig	Gene start	Gene end	Strand Expr.	Methylated Position	Strand Meth.	Distance Meth.	DE analysis				DM analysis				
										Direction	baseMean	LFC	P-value	Modification	mean % methylation: LiH	mean % methylation: ExH	% methylation difference	P-value
HMPREF1322_RS00725	-	lactate utilization protein	NZ_AJZS01000011.1	13105	14472	+	12945	+	-160	Under expr.	911.64	-2.93	5.26E-38	DMC	5.18%	61.79%	56.61%	2.71E-06
HMPREF1322_RS00725	-	lactate utilization protein	NZ_AJZS01000011.1	13105	14472	+	12946	+	-159	Under expr.	911.64	-2.93	5.26E-38	DMC	4.71%	58.08%	53.37%	2.09E-06
HMPREF1322_RS00725	-	lactate utilization protein	NZ_AJZS01000011.1	13105	14472	+	13002	+	-103	Under expr.	911.64	-2.93	5.26E-38	DMC	3.76%	55.38%	51.62%	3.63E-06
HMPREF1322_RS00725	-	lactate utilization protein	NZ_AJZS01000011.1	13105	14472	+	13071	+	-34	Under expr.	911.64	-2.93	5.26E-38	DMC	4.20%	21.99%	17.79%	4.48E-06
HMPREF1322_RS00725	-	lactate utilization protein	NZ_AJZS01000011.1	13105	14472	+	13178	+	73	Under expr.	911.64	-2.93	5.26E-38	DMC	7.08%	60.16%	53.08%	2.24E-06
HMPREF1322_RS00725	-	lactate utilization protein	NZ_AJZS01000011.1	13105	14472	+	13236	+	131	Under expr.	911.64	-2.93	5.26E-38	DMA	6.84%	52.42%	45.58%	5.83E-06
HMPREF1322_RS00725	-	lactate utilization protein	NZ_AJZS01000011.1	13105	14472	+	13240	+	135	Under expr.	911.64	-2.93	5.26E-38	DMC	8.76%	43.87%	35.12%	1.61E-06
HMPREF1322_RS00725	-	lactate utilization protein	NZ_AJZS01000011.1	13105	14472	+	13430	+	325	Under expr.	911.64	-2.93	5.26E-38	DMC	9.65%	38.76%	29.11%	2.55E-05
HMPREF1322_RS00725	-	lactate utilization protein	NZ_AJZS01000011.1	13105	14472	+	13584	+	479	Under expr.	911.64	-2.93	5.26E-38	DMA	2.40%	14.66%	12.25%	5.18E-07
HMPREF1322_RS00725	-	lactate utilization protein	NZ_AJZS01000011.1	13105	14472	+	13730	+	625	Under expr.	911.64	-2.93	5.26E-38	DMC	13.59%	58.15%	44.56%	1.13E-05
HMPREF1322_RS00725	-	lactate utilization protein	NZ_AJZS01000011.1	13105	14472	+	13965	+	860	Under expr.	911.64	-2.93	5.26E-38	DMA	3.83%	37.85%	34.02%	4.16E-06
HMPREF1322_RS00725	-	lactate utilization protein	NZ_AJZS01000011.1	13105	14472	+	14019	+	914	Under expr.	911.64	-2.93	5.26E-38	DMA	1.48%	34.21%	32.73%	1.48E-05
HMPREF1322_RS00725	-	lactate utilization protein	NZ_AJZS01000011.1	13105	14472	+	14106	+	1001	Under expr.	911.64	-2.93	5.26E-38	DMC	16.77%	47.36%	30.59%	7.45E-07
HMPREF1322_RS00725	-	lactate utilization protein	NZ_AJZS01000011.1	13105	14472	+	14200	+	1095	Under expr.	911.64	-2.93	5.26E-38	DMA	5.92%	18.54%	12.62%	8.66E-06
HMPREF1322_RS00725	-	lactate utilization protein	NZ_AJZS01000011.1	13105	14472	+	14323	+	1218	Under expr.	911.64	-2.93	5.26E-38	DMA	2.43%	19.81%	17.38%	1.65E-05
HMPREF1322_RS00725	-	lactate utilization protein	NZ_AJZS01000011.1	13105	14472	+	14324	+	1219	Under expr.	911.64	-2.93	5.26E-38	DMA	1.76%	17.10%	15.34%	3.75E-06
HMPREF1322_RS00725	-	lactate utilization protein	NZ_AJZS01000011.1	13105	14472	+	14487	+	1382	Under expr.	911.64	-2.93	5.26E-38	DMA	0.97%	19.32%	18.35%	2.62E-06
HMPREF1322_RS00725	-	lactate utilization protein	NZ_AJZS01000011.1	13105	14472	+	14511	+	1406	Under expr.	911.64	-2.93	5.26E-38	DMA	4.96%	46.35%	41.39%	3.60E-06
HMPREF1322_RS00725	-	lactate utilization protein	NZ_AJZS01000011.1	13105	14472	+	14512	+	1407	Under expr.	911.64	-2.93	5.26E-38	DMA	5.03%	41.65%	36.62%	1.56E-05
HMPREF1322_RS00725	-	lactate utilization protein	NZ_AJZS01000011.1	13105	14472	+	14542	+	1437	Under expr.	911.64	-2.93	5.26E-38	DMC	15.67%	34.20%	18.53%	8.76E-06
HMPREF1322_RS00725	-	lactate utilization protein	NZ_AJZS01000011.1	13105	14472	+	14644	+	1539	Under expr.	911.64	-2.93	5.26E-38	DMA	5.20%	29.07%	23.87%	4.28E-06
HMPREF1322_RS00725	-	lactate utilization protein	NZ_AJZS01000011.1	13105	14472	+	14669	+	1564	Under expr.	911.64	-2.93	5.26E-38	DMC	7.23%	19.84%	12.61%	1.28E-05
HMPREF1322_RS00725	-	lactate utilization protein	NZ_AJZS01000011.1	13105	14472	+	14693	+	1588	Under expr.	911.64	-2.93	5.26E-38	DMC	14.07%	38.73%	24.67%	1.77E-05
HMPREF1322_RS00725	-	lactate utilization protein	NZ_AJZS01000011.1	13105	14472	+	14698	+	1593	Under expr.	911.64	-2.93	5.26E-38	DMC	26.82%	44.78%	17.96%	7.90E-06
HMPREF1322_RS00725	-	lactate utilization protein	NZ_AJZS01000011.1	13105	14472	+	14706	+	1601	Under expr.	911.64	-2.93	5.26E-38	DMC	2.91%	21.70%	18.79%	1.52E-05
HMPREF1322_RS00725	-	lactate utilization protein	NZ_AJZS01000011.1	13105	14472	+	14744	+	1639	Under expr.	911.64	-2.93	5.26E-38	DMA	2.00%	28.52%	26.52%	1.52E-06
HMPREF1322_RS00725	-	lactate utilization protein	NZ_AJZS01000011.1	13105	14472	+	15471	+	2366	Under expr.	911.64	-2.93	5.26E-38	DMA	7.97%	28.75%	20.78%	1.11E-05
HMPREF1322_RS00730	-	hypothetical protein	NZ_AJZS01000011.1	14478	15062	+	13584	+	-894	Under expr.	1091.42	-3.38	5.01E-41	DMA	2.40%	14.66%	12.25%	5.18E-07

HMPREF1322_RS00730	-	hypothetical protein	NZ_AJZS01000011.1	14478	15062	+	13730	+	-748	Under expr.	1091.42	-3.38	5.01E-41	DMC	13.59%	58.15%	44.56%	1.13E-05
HMPREF1322_RS00730	-	hypothetical protein	NZ_AJZS01000011.1	14478	15062	+	13965	+	-513	Under expr.	1091.42	-3.38	5.01E-41	DMA	3.83%	37.85%	34.02%	4.16E-06
HMPREF1322_RS00730	-	hypothetical protein	NZ_AJZS01000011.1	14478	15062	+	14019	+	-459	Under expr.	1091.42	-3.38	5.01E-41	DMA	1.48%	34.21%	32.73%	1.48E-05
HMPREF1322_RS00730	-	hypothetical protein	NZ_AJZS01000011.1	14478	15062	+	14106	+	-372	Under expr.	1091.42	-3.38	5.01E-41	DMC	16.77%	47.36%	30.59%	7.45E-07
HMPREF1322_RS00730	-	hypothetical protein	NZ_AJZS01000011.1	14478	15062	+	14200	+	-278	Under expr.	1091.42	-3.38	5.01E-41	DMA	5.92%	18.54%	12.62%	8.66E-06
HMPREF1322_RS00730	-	hypothetical protein	NZ_AJZS01000011.1	14478	15062	+	14323	+	-155	Under expr.	1091.42	-3.38	5.01E-41	DMA	2.43%	19.81%	17.38%	1.65E-05
HMPREF1322_RS00730	-	hypothetical protein	NZ_AJZS01000011.1	14478	15062	+	14324	+	-154	Under expr.	1091.42	-3.38	5.01E-41	DMA	1.76%	17.10%	15.34%	3.75E-06
HMPREF1322_RS00730	-	hypothetical protein	NZ_AJZS01000011.1	14478	15062	+	14487	+	9	Under expr.	1091.42	-3.38	5.01E-41	DMA	0.97%	19.32%	18.35%	2.62E-06
HMPREF1322_RS00730	-	hypothetical protein	NZ_AJZS01000011.1	14478	15062	+	14511	+	33	Under expr.	1091.42	-3.38	5.01E-41	DMA	4.96%	46.35%	41.39%	3.60E-06
HMPREF1322_RS00730	-	hypothetical protein	NZ_AJZS01000011.1	14478	15062	+	14512	+	34	Under expr.	1091.42	-3.38	5.01E-41	DMA	5.03%	41.65%	36.62%	1.56E-05
HMPREF1322_RS00730	-	hypothetical protein	NZ_AJZS01000011.1	14478	15062	+	14542	+	64	Under expr.	1091.42	-3.38	5.01E-41	DMC	15.67%	34.20%	18.53%	8.76E-06
HMPREF1322_RS00730	-	hypothetical protein	NZ_AJZS01000011.1	14478	15062	+	14644	+	166	Under expr.	1091.42	-3.38	5.01E-41	DMA	5.20%	29.07%	23.87%	4.28E-06
HMPREF1322_RS00730	-	hypothetical protein	NZ_AJZS01000011.1	14478	15062	+	14669	+	191	Under expr.	1091.42	-3.38	5.01E-41	DMC	7.23%	19.84%	12.61%	1.28E-05
HMPREF1322_RS00730	-	hypothetical protein	NZ_AJZS01000011.1	14478	15062	+	14693	+	215	Under expr.	1091.42	-3.38	5.01E-41	DMC	14.07%	38.73%	24.67%	1.77E-05
HMPREF1322_RS00730	-	hypothetical protein	NZ_AJZS01000011.1	14478	15062	+	14698	+	220	Under expr.	1091.42	-3.38	5.01E-41	DMC	26.82%	44.78%	17.96%	7.90E-06
HMPREF1322_RS00730	-	hypothetical protein	NZ_AJZS01000011.1	14478	15062	+	14706	+	228	Under expr.	1091.42	-3.38	5.01E-41	DMC	2.91%	21.70%	18.79%	1.52E-05
HMPREF1322_RS00730	-	hypothetical protein	NZ_AJZS01000011.1	14478	15062	+	14744	+	266	Under expr.	1091.42	-3.38	5.01E-41	DMA	2.00%	28.52%	26.52%	1.52E-06
HMPREF1322_RS00730	-	hypothetical protein	NZ_AJZS01000011.1	14478	15062	+	15471	+	993	Under expr.	1091.42	-3.38	5.01E-41	DMA	7.97%	28.75%	20.78%	1.11E-05
HMPREF1322_RS00740	-	ABC transporter ATP-binding protein	NZ_AJZS01000011.1	16133	17839	-	15471	+	-662	Under expr.	7059.72	-2.68	5.06E-10	DMA	7.97%	28.75%	20.78%	1.11E-05
HMPREF1322_RS00740	-	ABC transporter ATP-binding protein	NZ_AJZS01000011.1	16133	17839	-	17614	+	1481	Under expr.	7059.72	-2.68	5.06E-10	DMA	2.76%	16.42%	13.66%	1.15E-05
HMPREF1322_RS00740	-	ABC transporter ATP-binding protein	NZ_AJZS01000011.1	16133	17839	-	18653	+	2520	Under expr.	7059.72	-2.68	5.06E-10	DMC	4.65%	18.69%	14.04%	2.34E-05
HMPREF1322_RS00745	-	ABC transporter ATP-binding protein	NZ_AJZS01000011.1	17886	19607	-	17614	+	-272	Under expr.	3619.54	-4.27	2.40E-57	DMA	2.76%	16.42%	13.66%	1.15E-05
HMPREF1322_RS00745	-	ABC transporter ATP-binding protein	NZ_AJZS01000011.1	17886	19607	-	18653	+	767	Under expr.	3619.54	-4.27	2.40E-57	DMC	4.65%	18.69%	14.04%	2.34E-05
HMPREF1322_RS00745	-	ABC transporter ATP-binding protein	NZ_AJZS01000011.1	17886	19607	-	19392	+	1506	Under expr.	3619.54	-4.27	2.40E-57	DMA	7.54%	25.19%	17.66%	1.14E-05
HMPREF1322_RS03650	-	4-alpha-glucanotransferase	NZ_AJZS01000038.1	2961	4847	-	3558	-	597	Under expr.	5951.7	-2.22	5.69E-14	DMC	5.53%	95.22%	89.69%	4.16E-07
HMPREF1322_RS03650	-	4-alpha-glucanotransferase	NZ_AJZS01000038.1	2961	4847	-	3559	-	598	Under expr.	5951.7	-2.22	5.69E-14	DMA	4.43%	89.64%	85.21%	7.67E-08
HMPREF1322_RS03650	-	4-alpha-glucanotransferase	NZ_AJZS01000038.1	2961	4847	-	3560	-	599	Under expr.	5951.7	-2.22	5.69E-14	DMA	1.45%	86.22%	84.77%	5.31E-06
HMPREF1322_RS06180	-	Ppx/GppA family phosphatase	NZ_AJZS01000066.1	22201	23108	-	22242	-	41	Over expr.	914.83	1.59	2.19E-12	DMA	15.95%	96.80%	80.86%	3.66E-07
HMPREF1322_RS06180	-	Ppx/GppA family phosphatase	NZ_AJZS01000066.1	22201	23108	-	22243	-	42	Over expr.	914.83	1.59	2.19E-12	DMC	10.21%	64.13%	53.91%	6.11E-07
HMPREF1322_RS06180	-	Ppx/GppA family phosphatase	NZ_AJZS01000066.1	22201	23108	-	22938	-	737	Over expr.	914.83	1.59	2.19E-12	DMA	85.99%	37.41%	48.59%	4.56E-06
HMPREF1322_RS06180	-	Ppx/GppA family phosphatase	NZ_AJZS01000066.1	22201	23108	-	22943	+	742	Over expr.	914.83	1.59	2.19E-12	DMC	70.43%	31.90%	38.53%	2.21E-05

Strand Expr: Strand of the gene

Strand Meth: Strand of the methylated position
Distance Meth: Distance of the methylated position to the gene start site in base pairs, negative values indicate upstream location
DE analysis: results from the differential expression analysis
DM analysis: results from the differential methylation analysis
LFC: log_2 fold change
LiH: growth in limited hemin
ExH: growth in excess hemin